VEP—FRD—33—A
OCTOBER, 1983

Vepco

REACTOR CORE THERMAL-HYDRAULIC ANALYSIS USING THE COBRA IIIC/MIT COMPUTER CODE

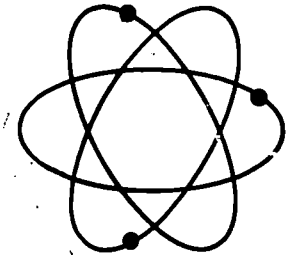

POWER STATION ENGINEERING DEPARTMENT
NUCLEAR FUEL ENGINEERING
VIRGINIA ELECTRIC AND POWER COMPANY

VEP-FRD-33-A

VEPCO REACTOR CORE THERMAL-HYDRAULIC ANALYSIS USING THE COBRA IIIC/MIT COMPUTER CODE

BY
F. W. SLIZ
K. L. BASEHORE

NUCLEAR FUEL ENGINEERING GROUP
POWER STATION ENGINEERING DEPARTMENT

VIRGINIA ELECTRIC AND POWER COMPANY
RICHMOND, VIRGINIA

OCTOBER, 1983

RECOMMENDED FOR APPROVAL:

R. W. Cross
Supervisor, Nuclear Fuel Engineering

APPROVED:

R. M. Berryman
Director, Nuclear Fuel Engineering

UNITED STATES
NUCLEAR REGULATORY COMMISSION
WASHINGTON, D. C. 20555

AUG 2 6 1983

Mr. R. H. Leasburg, Vice President
Nuclear Operations
Virginia Electric & Power Company
Richmond, Virginia 23261

Dear Mr. Leasburg:

Subject: Acceptance for Referencing of Licensing Topical Report VEP-FRD-33, "VEPCO Reactor Core Thermal-Hydraulic Analysis Using the COBRA-IIIC/MIT Computer Code"

We have completed our review of the subject topical report submitted September 28, 1979 by Virginia Electric and Power Company (VEPCO) letter Serial No. 795. We find this report is acceptable for referencing in license applications to the extent specified and under the limitations delineated in the report and the associated NRC evaluation which is enclosed. The evaluation defines the basis for acceptance of the report.

We do not intend to repeat our review of the matters described in the report and found acceptable when the report appears as a reference in license applications except to assure that the material presented is applicable to the specific plant involved. Our acceptance applies only to the matters described in the report.

In accordance with procedures established in NUREG-0390, it is requested that VEPCO publish accepted versions of this report, proprietary and non-proprietary, within three months of receipt of this letter. The accepted versions should incorporate this letter and the enclosed evaluation between the title page and the abstract. The accepted versions shall include an -A (designating accepted) following the report identification symbol.

Should our criteria or regulations change such that our conclusions as to the acceptability of the report are invalidated, VEPCO and/or the applicants referencing the topical report will be expected to revise and resubmit their respective documentation, or submit justification for the continued effective applicability of the topical report without revision of their respective documentation.

Sincerely,

Cecil O. Thomas

Cecil O. Thomas, Chief
Standardization & Special
Projects Branch
Division of Licensing

Enclosure:
As stated

TOPICAL REPORT EVALUATION

Report Title:	Virginia Electric & Power Company Reactor Core Thermal-Hydraulic Analysis Using the COBRA IIIC/MIT Computer Code
Report Number:	VEP-FRD-33
Report Date:	August 1979
Responsible Branch:	Standardization and Special Projects
DSI Branch Involved:	Core Performance Branch

Introduction

This report describes the Virginia Electric & Power Company (VEPCO) thermal-hydraulic model and its application to VEPCO's pressurized water reactor cores (i.e., North Anna, Surry). The accuracy of the VEPCO thermal-hydraulic model is demonstrated through comparisons with analyses which were used in the design and licensing of the Surry Nuclear Power Station. VEPCO has also submitted a number of check cases (Ref. 2), some of which have been compared to staff audit calculations, to further demonstrate the accuracy of their model.

VEPCO Thermal-Hydraulic Model

VEPCO's thermal-hydraulic model is an adaptation of the COBRA IIIC/MIT (Ref. 1). The major modifications to COBRA IIIC/MIT include:

1. The capability to do the thermal hydraulic analysis using single stage method which incorporates the geometries and methodologies used in traditional multistage analyses.

2. The two phase density in the subcooled void region is based upon the saturated vapor and subcooled liquid densities.

3. The DNBRs are printed out by channel numbers instead of rod numbers.

4. The W-3 L-grid and R-grid spacer factor correlations are options available in the code.

5. The fraction of the heat generated in the fuel and cladding are accounted for in the CHF calculations.

6. The calculation iterates at least twice before convergence but includes a variable damping factor input for more rapid convergence.

7. An option is added so that different crossflow resistance and mixing coefficients could be input and applied to the rod gaps.

8. Up to six different axial heat flux shapes could be input and applied to different fuel rods.

9. All water properties (enthalpy, specific volume, viscosity, conductivity and specific heat) are calculated using the HOH routines which are obtained from the PDQ7V2 computer code.

10. Saturated liquid properties are used to correct the calculations of the true (non-equilibrium) quality within the Levy subcooled model.

Description

The COBRA-IIIC/MIT computer code calculates the flow and enthalpy within interconnected flow channels by solving finite difference equations of continuity, energy, and momentum. The mathematical model is applicable to both steady state and transient conditions and the model considers both turbulent mixing and diversion crossflow. In formulating the model one-dimensional, two-phase, separated, slip-flow is assumed to exist during boiling. The two-phase flow structure is assumed to be fine enough to specify the void fraction as a function of enthalpy, flow rate, heat flux, pressure, position, and time. Sonic velocity propagation effects are not included. Within a channel, the diversion crossflow velocity is assumed to be small compared to the axial velocity to allow the use of a simplified equation for the conservation of transverse momentum.

The same finite difference equations are used for both steady state and transient computations. Initial conditions are obtained by performing a steady state calculation and then transient calculation is performed. Time dependent forcing functions consisting of inlet temperature, inlet flow, system pressure, and core average heat flux are used to establish boundary conditions at succeeding times. The calculation iterates over the first time step until the flow solution converges. The converged solution is then used as the initial condition for the new time, and the procedure continues for all the subsequent time steps. The correlations used in calculating turbulent mixing are of major importance. Once the flow solution is obtained, additional correlations are used in calculating the DNBR distribution. The COBRA-IIIC/MIT computer code allows user specification of the appropriate correlations.

Models and Correlations

The void fractions are predicted using the Smith correlation (Ref. 3) in conjunction with the Levy subcooled model (Ref. 4). In computing single and two-phase pressure drops, an isothermal friction factor correlation is used in conjunction with a wall viscosity correlation and a correlation for predicting two-phase friction multipliers.

In predicting the non-uniform critical heat flux, the W-3 correlation is used in conjunction with the F-factor correlation (Ref. 5). In determining the lower bound of the F-factor integral, the Jens and Lottes correlation (Ref. 6) is used to predict the axial position where nucleate boiling begins. When appropriate, the coldwall factor and the L-grid or R-grid spacer factor (Ref. 7) are used with the W-3 correlation to predict the critical heat flux.

Turbulent Mixing

The degree of turbulent mixing between adjacent channels is calculated using the following relationship,

$$w' = \beta \, sG$$

where w' is the turbulent transverse fluctuating flow rate per axial length, G is the average mass velocity of the adjacent channels, s is the common gap, and β is the mixing coefficient. The above relationship is used to predict both single and two-phase mixing.

Hydraulic Model Description

Eighth core symmetry is assumed, and thus 1/8 core segment is modeled. The location of hot assembly is assumed at the center of the core. The hot assembly is modeled as an array of subchannels, while the remaining assemblies are modeled as an array of lumped channels. For steady state analysis, a fine mesh geometry is used in which each lumped assembly and each hot assembly subchannel is modeled as an individual flow channel. For transient analysis, a coarse mesh geometry is used in which assemblies and subchannels are combined to form large channels. Because the coarser geometry contains fewer channels, less computational time per iteration will be required for the transient analysis.

A 53 channel model has been developed for steady state analysis and a 19 channel model has been developed for transient analysis of the Surry units. This 53 channel model consisted of 25 lumped assembly channels and 28 subchannels. The 19 channel model consisted of 4 lumped channels and 15 subchannels.

Thermal Model Description

The thermal model consists of an inlet flow distribution, radial and axial power distributions, and appropriate reactor operating conditions. For transient analysis, time dependent forcing functions of system pressure, inlet flow, inlet temperature, and core average heat flux are also specified.

Thermal hydraulic design parameters form the basis of the model. The radial power distribution is based upon the design value of $F^N_{\Delta H}$, and the axial power distribution is based on the reference axial shape. The thermal design flow rate is used in determining the core average mass velocity, and the thermal hydraulic design values for inlet temperature, system pressure, and power level are used as operating conditions.

The thermal model is then imposed upon the hydraulic model in order to obtain the complete thermal-hydraulic representation of the core. Since this representation is dependent upon thermal-hydraulic design parameters, revised representations must be considered in the event of any subsequent design changes. In general, the hydraulic model remains relatively fixed since it is affected only by changes in the mechanical design of the fuel. However, the thermal model can be significantly affected by changing any one of the design parameters.

Inlet Flow Distribution

The inlet flow distribution used in the 53 channel model for steady state analyses and 19 channel model for transient analyses, assumes a 5 percent flow reduction to the hot assembly while the peripheral assemblies have a flow fraction slightly greater than 1.0. Therefore, the average of all the fractions is approximately 1.0.

Power Distribution

The hot assembly as well as the adjacent assemblies are given relative powers of 1.475, while lower relative powers are assigned to the remaining assemblies. The average of all the assembly relative powers is 1.0. The assembly power distribution for the 19 channel model is derived from the 53 channel model by averaging all but the three central assembly powers. Within the subchannel array, a second power gradient exists, having a peak around the hot channel which is a thimble cell. The three fuel rods surrounding the hot thimble cell have relative powers of 1.55, the remaining fuel rods are at lower relative powers. The average of all the fuel rod relative powers is equal to the hot assembly relative power, 1.475.

The subchannel power distribution for the 19 channel model is also derived from the 53 channel model by averaging the relative power of the fuel rods located within the lumped subchannel. The same axial power distribution is used in both the 19 and 53 channel models.

Forcing Functions for Transient Analysis

For each reactor parameter that is changing with time, a forcing function is input as a table set with each entry consisting of the ratio of the transient condition to the initial condition and a corresponding time. The COBRA-IIIC/MIT computer code has the capability of handling four different forcing functions, e.g., core average heat flux vs time, inlet flow vs time, inlet temperature vs time, and system pressure vs time.

Engineering Uncertainties

After formulating the overall thermal-hydraulic representation of the core, engineering uncertainties are then applied to account for manufacturing tolerances used in the fabrication of the fuel. These fabrication tolerances are assumed to occur in the hot channel, and are called hot channel factors.

These factors consist of a pitch reduction, an engineering factor on the enthalpy rise ($F^E_{\Delta H}$), and an engineering factor on the heat flux (F^E_Q). The pitch reduction takes into account fuel rod spacing variations which may occur within the as-built fuel assembly. This reduced pitch is accounted for by modeling the hot channel with reduced gap spacing and a reduced flow area. Since a reduced flow area causes a greater pressure loss across the spacer grids, this effect is taken into account by using increased grid loss coefficients. Table 1 lists the hydraulic data which was used in modeling the hot channel.

The engineering factor of the enthalpy rise ($F^E_{\Delta H}$) takes into account the effect of enrichment and density variations which may occur in as-built fuel rods. This factor is accounted for by increasing the relative power of the hot fuel rod. For all the DNB analyses described within this report, the relative power of the hot fuel rod was multiplied by a factor of 1.02.

TABLE 1

HOT CHANNEL HYDRAULIC DATA

Hot Thimble Cell	
Pitch Reduction (inches)	0.0065
Reduced Flow Area (square inches)	0.1463
Reduced Fuel Rod to Fuel Rod Gap (inches)	0.1345
Reduced Fuel Rod to Thimble Tube Gap (inches)	0.0725
Hot Unit Cell	
Pitch Reduction (inches)	0.0065
Reduced Flow Area (square inches)	0.1698
Reduced Fuel Rod to Fuel Rod Gap (inches)	0.1345

The engineering factor on the heat flux (F_Q^E) takes into account the effect of enrichment, density, diameter, and eccentricity variations which may occur in as-built fuel pellets. This factor is accounted for by applying a heat flux spike on the hot fuel rod at the position of MDNBR. Before the heat flux spike can be applied, however, a thermal analysis must first be performed in order to determine the axial position of MDNBR. Based upon these results, the axial heat flux shape for the hot fuel rod is then adjusted to include a heat flux spike at the determined position. The spike flux shape is included in a second thermal analysis from which the final results are obtained.

An engineering factor on the heat flux was applied to all the DNB analyses described in reference 1.

Thermal-Hydraulic Model Verification

VEPCO performed three steady state and six transient DNB analyses to verify the calculational accuracy of their thermal-hydraulic model. These analyses are listed in Table 2, and are representative of those contained in the original Surry FSAR and in subsequent licensing documents that update the FSAR. The minimum DNBRs obtained from the VEPCO model were compared to the values in the licensing documents. These values are provided in Table 3. This comparison results show that the VEPCO model to be consistant with previously submitted and approved licensing documents.

Staff Evaluation

Although VEPCO's original analyses showed fairly good agreement with the Surry FSAR calculations, the staff was still concerned that since the VEPCO code uses a single-pass method it should be benchmarked directly against a multi-pass code for a range of operating conditions. In response to concerns of the staff, VEPCO submitted (Ref. 2) the 7 check cases listed in Table 6. These cases are one for one comparisons

TABLE 2

LISTING OF VEPCO VERIFICATION ANALYSES

FSAR[8] Analyses

Steady State at 100% Power

Excessive Load Increase Transient

Uncontrolled Control Rod Assembly Withdrawal at Power Transient

Complete Loss of Reactor Coolant Flow Transient

Densification[9]/Positive Moderator Temperature Coefficient[10,11] Reanalyses

Steady State at 112% Power

Uncontrolled Control Rod Assembly Withdrawal At Power Transient

Complete Loss of Reactor Coolant Flow Transient

Low Flow Assumption[12] Reanalyses

Steady State at 102% Power

Complete Loss of Reactor Coolant Flow Transient

TABLE 3

	MDNBR		
	Surry FSAR	VEPCO	Channel Model
FSAR			
SS @ 100% Power	1.97	1.94 1.94	53 19
Excessive Load Increase Transient	1.55	1.53	19
Uncontrolled Control Rod Assembly Withdrawal	1.36	1.24	19
Complete Loss of RC Flow	1.46	1.48	-
Ref. 10	Ref. 10	VEPCo	
SS @ 112% Power	1.30	1.30 1.27	53 19
Uncontrolled	1.32	1.36	19
Complete loss of RC Flow	1.54	1.54	-
Low Flow Assumption Reanalysis Ref. 12			
SS @ 102% Power	1.50	1.49 1.49	53 19
Complete Loss of RC Flow Transient	1.33	1.35	-

TABLE 4

Range of Key Test Parameters

	Ranges
Pressure (psia)	1491-2433
Inlet Average Mass Velocity (Mlbm/hr-ft^2)	1.05-3.66
Inlet Temperature (°F)	433.0-617.0
Local Heat Flux (MBTU/hr-ft^2)	0.563-1.063

TABLE 5

W-3 Correlation Limits

Correlation	Ref. No.	Pressure Range (psia)	Mass Velocity (Mlb/h-ft²)	Equiv. Diameter (in)	Local Quality	Axial Height (in)	Inlet Temp (°F)
W-3	1,2	1000-2400	1.0-5.0	0.2-0.7	≤0.15	10-144	>400
F-factor	1,2	1000-2400	1.0-3.0	0.2-0.7	≤0.15	10-144	
Coldwall Factor	1,2 3,4	1000-2400	1.0-5.0		≤0.15	>10	
Spacer Factor	3,4	1490-2440	1.5-3.7		≤0.15	96-168	404-624

TABLE 6

SUMMARY OF COMPARISONS WITH THINC-I

Case No.	Pressure (psia)	Power (%)	Flow (%)	Tin (°F)	FΔH	Axial Offset	Minimum DNBR COBRA	Minimum DNBR THINC- I
1	2200.	112.	100.	554.	1.24	zero	1.27	1.30
2	2400.	118.	100.	563.	1.03	zero	1.30	1.33
3	2400.	101.	100.	563.	1.03	large positive	1.32	1.39
4	2400.	81.7	100.	618.4	1.03	large negative	1.30	1.33
5	1855.	112.	90.	515.	1.03	zero	1.47	1.47
6	2220.	100.5	76.5	547.	1.03	zero	1.32	1.32
7	2400.	101.	100.	563.	1.03	large positive	1.42	1.50

between the COBRA 19 channel single-pass and the THINC-I multi-pass 1/8 core models. These cases were chosen to span the general licensed operating range of the VEPCO plants. A consistent set of input was used for both computer codes.

Case 1 is a recalculation of the VEP-FRD-33 Section 6.3.2 state-point. It represents a point on the 2200 psi core thermal limit line at 112 percent power and conditions based on the densification/positive moderator temperature coefficient reanalysis.

Case 2 computes a point which would exist on a COBRA generated 2400 psia core thermal limit line at 118 percent power. Thermal design flow and the currently applicable heat flux spike were used.

Case 3 is a recomputation of Case 2, using a large positive axial offset power distribution instead of the normal cosine shaped axial power distribution. The power was adjusted to yield a COBRA minimum DNBR approximately equal to 1.30 (the actual value is 1.32). This set of operating conditions was then applied to the THINC-I calculation.

Case 4 shows the effect of reduced power and a large negative axial offset power distribution. As in Case 4, the power was adjusted to yield a COBRA minimum DNBR approximately equal to 1.30.

Case 5 shows the effect of reduced pressure and flow. This state-point corresponds to conditions on the existing Surry 1855 psia core thermal limit line at 112 percent power. Current fuel stack height reduction and heat flux spike factors were used in this calculation, as opposed to the densification reanalysis values used in the limit line generation.

Case 6 shows the effect of reduced flow. The loss-of-flow transient reported in VEP-FRD-33 Section 6.4.3 was rerun with COBRA using corrected values for reduced fuel height and heat flux spike to yield minimum DNBR results identical to those from THINC-III.

Case 7 is the same as Case 3 except a different axial power distribution was used.

In all these cases the COBRA 19 channel single-pass model yielded either identical or conservative minimum DNBR's when compared with the THINC-I multi-pass model results.

As part of our review, the staff chose Cases 1 and 7 to perform audit calculations of VEPCO methodology using COBRA-IV. Our analyses were performed in two steps. First, an eighth core symmetric core-wide calculation was performed to determine the flow to the hot assembly. This crossflow was stored on tape and used as a boundary condition in the subchannel calculations. For the subchannel case, an octant of the limiting assembly was modeled on a rod-by-rod basis. The cases selected were those that had the greatest deviation between COBRA-IIIC/MIT and THINC-I. Table 7 contains the operating conditions for the cases analyzed while Table 8 presents a comparison of the results.

From Table 8, it can be seen that there is good agreement between the staff's detailed audit calculations and VEPCO's COBRA-IIIC/MIT results. In both cases, VEPCO is conservative when compared to our results.

TABLE 7

OPERATING CONDITIONS

Power Shape	Peak Value	Pressure (Psia)	T_{IN} (^{o}F)	Average 9" (MBTU/hr-ft^2)	Mass Velocity (MLBM/hr-ft^2)
Cosine	1.550	2200.0	554.0	0.22231	2.273
Upskew	1.748	2400.0	563.0	0.20000	2.251

TABLE 8

CALCULATIONAL RESULTS

Power Shape	VEPCo COBRA-IIIC/MIT	THINC-I	NRC COBRA-IV
Cosine	1.27	1.30	1.33
Upskew	1.42	1.50	1.53

Summary

In order to verify the calculational accuracy of their thermal-hydraulic model, VEPCO initially performed steady state and transient DNB analyses duplicating their original Surry FSAR analyses. This comparison showed the VEPCO model to be consistent with previously submitted and approved licensing documents. In addition, VEPCO submitted 7 check cases comparing their model on a one for one basis with the THINC-I multi-pass 1/8 core model. In all these cases the VEPCO model yielded either identical or conservative minimum DNBRs. Finally, the staff performed audit calculations of the VEPCO analyses using COBRA-IV. These audit calculations showed VEPCO's analyses to be both consistent and conservative relative to the staff's results.

Based on the staff review of the methodology presented in reference 1 and on the verification analyses performed by VEPCO and the staff, the staff finds reference 1 to be acceptable for referencing by VEPCO in future reload licensing submittals for North Anna, Surry and future plants of the same design.

FIGURE 1

COMPARISON OF DNB DATA WITH COBRA PREDICTIONS

Heated Length	Axial Flux Distribution	Grid with Vane	Grid without Vane
8'	u sin u cosine u	● ○	▲ –
14'	u sin u cosine u	■ ◇	– –

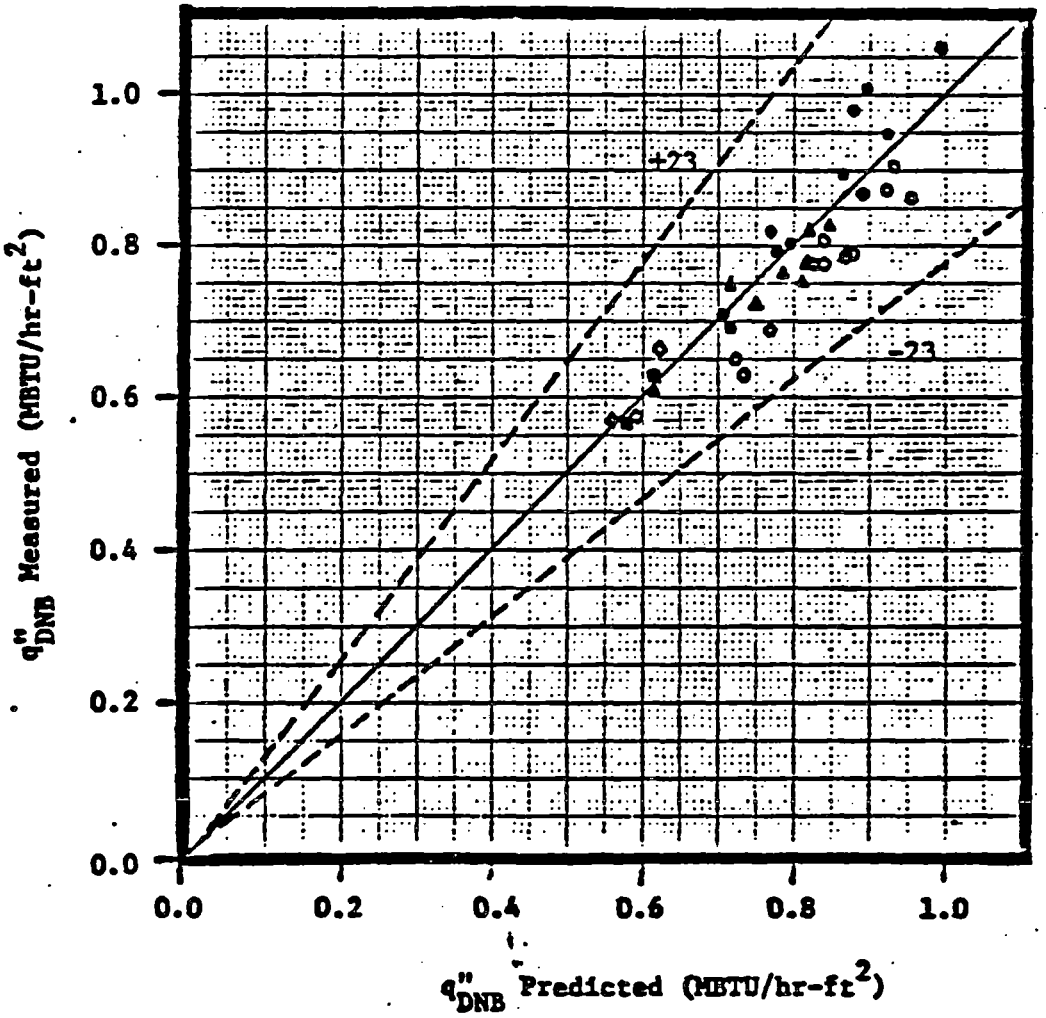

References

1. F. W. Suz, "VEPCO Reactor Core Thermal-Hydraulic Analysis Using the COBRA-IIIC/MIT Computer Code," VEP-FRD-33, Virginia Electric & Power Company, August 1979.

2. Letter from R. H. Leasburg (VEPCO) to H. R. Denton, October 4, 1982.

3. S. L. Smith, "Void Fractions in Two-Phase Flow: A Correlation Based Upon an Equal Velocity Head Model," Proceeding of the Institution of Mechanical Engineers, Volume 184, Part 1, No. 36, P. 647 (1969-70).

4. S. Levy, "Forced Convection Subcooled Boiling - Prediction of Vapor Volumetric Fraction," GEAP-5157, General Electric Company, April 1966.

5. L. S. Tong, "Boiling Crisis and Critical Heat Flux," TID-25887, U.S. Atomic Energy Commission, 1951.

6. W. H. Jens and P. A. Lottes, "Analyses of Heat Transfer, Burnout, Pressure Drop, and Density Data for High Pressure Water," USAEC Report ANL-4627, Argonne National Laboratory, 1951.

7. F. F. Cadek and F. E. Motley, "Application of Modified Spacer Factor to L. Grid Typical and Coldwall Cell DNB," WCAP-8030-A, Westinghouse Electric Corporation, January 1975.

8. FSAR - Surry Power Station Units 1 and 2, VEPCO (December 1969).

9. "Fuel Densification - Surry Power Station Unit 1," WCAP-8012, Westinghouse Electric Corporation (December 1972), Proprietary.

10. VEPCO (C. M. Stallings) to NRC (K. R. Goller) letter dated June 5, 1975, Serial No. 553, Docket Nos. 50-280 and 50-281.

11. VEPCO (C. M. Stallings) to NRC (B. C. Rusche) letter dated January 29, 1976, Serial No. 876, Docket Nos. 50-280 and 50-281.

12. VEPCO (C. M. Stallings) to NRC (E. G. Case) letter dated August 9, 1977, Serial No. 344, Docket Nos. 50-280 and 50-281.

CLASSIFICATION/DISCLAIMER

The data, information, analytical techniques, and conclusions in this report have been prepared solely for use by the Virginia Electric and Power Company (the Company), and they may not be appropriate for use in situations other than those for which they were specifically prepared. The Company therefore makes no claim or warranty whatsoever, express or implied, as to their accuracy, usefulness, or applicability. In particular, THE COMPANY MAKES NO WARRANTY OF MERCHANTABILITY OR FITNESS FOR A PARTICULAR PURPOSE, NOR SHALL ANY WARRANTY BE DEEMED TO ARISE FROM COURSE OF DEALING OR USAGE OF TRADE, with respect to this report or any of the data, information, analytical techniques, or conclusions in it. By making this report available, the Company does not authorize its use by others, and any such use is expressly forbidden except with the prior written approval of the Company. Any such written approval shall itself be deemed to incorporate the disclaimers of liability and disclaimers of warranties provided herein. In no event shall the Company be liable, under any legal theory whatsoever (whether contract, tort, warranty, or strict or absolute liability), for any property damage, mental or physical injury or death, loss of use of property, or other damage resulting from or arising out of the use, authorized or unauthorized, of this report or the data, information, analytical techniques, or conclusions in it.

ABSTRACT

The Virginia Electric and Power Company (VEPCO) has developed the capability to perform core thermal-hydraulic analysis using the COBRA IIIC/MIT computer code. This capability is based upon a single stage method of analysis which incorporates the geometries and methodologies used in traditional multistage analyses. Using the single stage approach, an array of subchannels representing the hot assembly is combined with an array of lumped channels which represent the remaining assemblies within an eighth core segment. Axial and radial design power distributions along with an inlet flow distribution are applied to this geometry, and engineering uncertainties are applied to the hot channel and the hot fuel rod. This thermal-hydraulic representation of the core is then used in a single thermal analysis to determine hot channel fluid conditions and the resulting minimum departure from nucleate boiling ratio (MDNBR).

The accuracy of the VEPCO Thermal-Hydraulic Model is demonstrated through comparisons with analyses which were used in the design and licensing of the Surry Nuclear Power Station. Steady state and transient MDNBRs calculated using the VEPCO methods are in excellent agreement with those presented in the licensing documents.

ACKNOWLEDGEMENTS

I would like to acknowledge the work of the following persons: H.S. BERMAN for programming an operational version of the COBRA IIIC/MIT computer code; M.L. SMITH, N.P. WOLFHOPE, and S.M. MIRSKY for assisting in the development of the Thermal-Hydraulic Model; Ms. CATHY BULLOCK, Ms. MARLENE SIMMS, Ms. MARY MOSS, and Ms. MIRANDA COOPER for typing the draft and final manuscripts. I would also like to thank a number of people who reviewed and provided comments on this report.

TABLE OF CONTENTS

Page

CLASSIFICATION/DISCLAIMER i

ABSTRACT ii

ACKNOWLEDGMENTS iii

TABLE OF CONTENTS iv

LIST OF FIGURES vi

LIST OF TABLES viii

SECTION 1 - INTRODUCTION 1-1

SECTION 2 - COBRA IIIC/MIT COMPUTER CODE DESCRIPTION 2-1

2.1 Introduction 2-1
2.2 Method of Solution 2-1
2.3 Models and Correlations 2-3
2.3.1 Void Fraction 2-3
2.3.2 Single and Two-Phase Friction Factors 2-3
2.3.3 Turbulent Mixing 2-4
2.3.4 Critical Heat Flux Correlation 2-5
2.3.5 Water Properties 2-5
2.4 Computational Input Parameters 2-5

SECTION 3 - HYDRAULIC MODEL DESCRIPTION 3-1

3.1 Introduction 3-1
3.2 General Description of the Surry Core 3-1
3.3 Eighth Core Representation - 53 Channel Model 3-2
3.4 Eighth Core Representation - 19 Channel Model 3-3

SECTION 4 - THERMAL MODEL DESCRIPTION 4-1

4.1 Introduction 4-1
4.2 General Description of the Thermal-Hydraulic Design of the Surry Core 4-2
4.3 Inlet Flow Distribution 4-3
4.4 Power Distribution 4-4
4.5 Reactor Operating Conditions 4-5
4.6 Forcing Functions for Transient Analysis 4-7

SECTION 5 - ENGINEERING UNCERTAINTIES 5-1

5.1 Introduction 5-1
5.2 Hot Channel Factors 5-1

SECTION 6 - THERMAL-HYDRAULIC MODEL VERIFICATION 6-1

6.1 Introduction 6-1
6.2 FSAR Analyses 6-3
6.2.1 Introduction 6-3
6.2.2 Steady State Analysis at 100% Power 6-3
6.2.3 Excessive Load Increase Transient 6-4

TABLE OF CONTENTS (Continued)

Page

6.2.4 Uncontrolled Control Rod Assembly Withdrawal at Power Transient 6-4
6.2.5 Complete Loss of Reactor Coolant Flow Transient 6-5
6.3 Densification/Positive Moderator Temperature Coefficient Reanalyses 6-16
6.3.1 Introduction 6-16
6.3.2 Steady State Analysis at 112% Power 6-16
6.3.3 Uncontrolled Control Rod Assembly Withdrawal at Power Transient 6-17
6.3.4 Complete Loss of Reactor Coolant Flow Transient 6-17
6.4 Low Flow Assumption Reanalyses 6-29
6.4.1 Introduction 6-29
6.4.2 Steady State Analysis at 102% Power 6-29
6.4.3 Complete Loss of Reactor Coolant Flow Transient 6-30

SECTION 7 - SUMMARY AND CONCLUSIONS 7-1

SECTION 8 - REFERENCES 8-1

APPENDIX A - VEPCO MODIFICATIONS ADDED TO THE COBRA IIIC/MIT COMPUTER CODE A-1

LIST OF FIGURES

Figure	Title	Page
3-1	Fuel Assembly Arrangement of Surry Core	3-10
3-2	Cross Sectional View of Surry Fuel Assembly	3-11
3-3	Side View of Surry Fuel Assembly	3-12
3-4	Assembly Geometry of 53 Channel Model	3-13
3-5	Subchannel Geometry of 53 Channel Model	3-14
3-6	Assembly Geometry of 19 Channel Model	3-15
3-7	Subchannel Geometry of 19 Channel Model	3-16
4-1	Inlet Flow Distribution of 53 Channel Model	4-9
4-2	Inlet Flow Distribution of 19 Channel Model	4-10
4-3	Assembly Power Distribution, 53 Channel Model, (Low Flow Assumption Reanalysis)	4-11
4-4	Assembly Power Distribution, 19 Channel Model, (Low Flow Assumption Reanalysis)	4-12
4-5	Subchannel Power Distribution, 53 Channel Model, (Low Flow Assumption Reanalysis)	4-13
4-6	Subchannel Power Distribution, 19 Channel Model, (Low Flow Assumption Reanalysis)	4-14
6-1	Assembly Power Distribution, 53 Channel Model, FSAR Analysis	6-9
6-2	Assembly Power Distribution, 19 Channel Model, FSAR Analysis	6-10
6-3	Subchannel Power Distribution, 53 Channel Model, FSAR Analysis	6-11
6-4	Subchannel Power Distribution, 19 Channel Model, FSAR Analysis	6-12
6-5	DNBR vs. Time, Excessive Load Increase Transient, FSAR Analysis	6-13
6-6	DNBR vs. Time, Uncontrolled Control Rod Assembly Withdrawal at Power Transient, FSAR Analysis	6-14

LIST OF FIGURES (Continued)

Figure	Title	Page
6-7	DNBR vs. Time, Complete Loss of Reactor Coolant Flow Transient, FSAR Analysis	6-15
6-8	Assembly Power Distribution, 53 Channel Model, Densification/Positive Moderator Temperature Coefficient Reanalysis	6-22
6-9	Assembly Power Distribution, 19 Channel Model, Densification/Positive Moderator Temperature Coefficient Reanalysis	6-23
6-10	Subchannel Power Distribution, 53 Channel Model, Densification/Positive Moderator Temperature Coefficient Reanalysis	6-24
6-11	Subchannel Power Distribution, 19 Channel Model, Densification/Positive Moderator Temperature Coefficient Reanalysis	6-25
6-12	Reactor Core Thermal and Hydraulic Safety Limit Curve at 2200 PSIA, Three Loop Operation, 100% Flow	6-26
6-13	DNBR vs. Time, Uncontrolled Control Rod Assembly Withdrawal at Power Transient, Positive Moderator Temperature Coefficient Reanalysis	6-27
6-14	DNBR vs. Time, Complete Loss of Reactor Coolant Flow Transient, Positive Moderator Temperature Coefficient Reanalysis	6-28
6-15	DNBR vs. Time, Complete Loss of Reactor Coolant Flow Transient, Low Flow Assumption Reanalysis	6-33

LIST OF TABLES

Table	Title	Page
2-1	Computational Input Parameters	2-6
3-1	Assembly Hydraulic Parameters	3-4
3-2	Axial Positions of Assembly Components	3-5
3-3	Assembly Hydraulic Data	3-6
3-4	Unit Cell Hydraulic Data	3-6
3-5	Perimeter Cell Hydraulic Data	3-6
3-6	Corner Cell Hydraulic Data	3-7
3-7	Thimble Cell Hydraulic Data	3-7
3-8	Hydraulic Data for Lumped Channels	3-8
4-1	Axial Power Distribution, (Low Flow Assumption Reanalysis)	4-8
5-1	Hot Channel Hydraulic Data	5-3
6-1	Listing of VEPCO Verification Analyses	6-2
6-2	Axial Power Distribution, FSAR Analysis	6-6
6-3	Reactor Conditions, FSAR Analysis	6-7
6-4	Parameters for FSAR Analysis	6-8
6-5	Axial Power Distribution, Densification/Positive Moderator Temperature Coefficient Reanalysis	6-19
6-6	Reactor Conditions, Densification/Positive Moderator Temperature Coefficient Reanalysis	6-20
6-7	Parameters for Densification/Positive Moderator Temperature Coefficient Reanalysis	6-21
6-8	Reactor Conditions, Low Flow Assumption Reanalysis	6-31
6-9	Parameters for Low Flow Assumption Reanalysis	6-32
7-1	Summary of Comparisons	7-2

SECTION 1 - INTRODUCTION

The basic objective of core thermal-hydraulic analysis is the accurate calculation of coolant conditions in order to verify that the fuel assemblies constituting the reactor core can safely meet the limitations imposed by departure from nucleate boiling (DNB). DNB, which could occur on the heating surface of the fuel rod, is characterized by a sudden decrease in the heat transfer coefficient with a corresponding increase in the surface temperature. DNB is of concern in reactor design because of the possibility of fuel rod failure resulting from the increased temperature.

In order to preclude potential DNB related fuel damage, a design basis is established and is expressed in terms of a minimum departure from nucleate boiling ratio (MDNBR). DNBR is the ratio of the predicted heat flux at which DNB occurs (i.e., the critical heat flux, CHF) and the local heat flux of the fuel rod. By imposing a design DNBR limit, adequate heat transfer between the fuel cladding and the reactor coolant is assured. DNBRs greater than the design limit indicate the existence of thermal margin within the nuclear core. Thus, the purpose of core thermal-hydraulic analysis, or DNB analysis, is the accurate calculation of DNBRs in order to assess and quantify core thermal margin.

In performing DNB analysis, a subchannel approach is commonly used wherein a section of the core is modeled as an array of adjoining subchannels. Each subchannel is defined as the flow channel formed by four fuel rods, or by three fuel rods and a guide thimble tube. When the fuel rods are given design radial and axial power distributions, the array represents the region of maximum design power generation. Within this array, the hottest subchannel (hot channel) is identified with the fuel rod which has the highest integrated

power (hot fuel rod). Engineering uncertainties are applied to the hot channel and the hot fuel rod in order to conservatively account for manufacturing tolerances. A detailed thermal analysis of the core is then performed to determine the flows and enthalpies at each axial position within the hot channel.

When performing the thermal analysis, it is necessary to consider the effect that the surrounding core region has on the subchannel flows. The problem is basically one of integrating the relatively small subchannel geometry into a larger geometry which is representative of the entire core. Traditionally, the problem has been solved by using a multistage method involving at least two analyses[1,2,3,4]. In general, a core analysis is first performed to provide crossflow boundary conditions which are used in the subsequent subchannel analysis. In the core analysis, each fuel assembly is modeled as a single, lumped flow channel. In the subchannel analysis, the hot assembly is modeled separately as an array of subchannels. Hot assembly crossflows determined in the first analysis are used as boundary conditions in the second analysis in order to simulate the effects of the core on the subchannel flows.

An alternate, more direct approach for performing the thermal analysis is a single stage method.[5] Using this method, a single analysis is performed in which an array of subchannels representing the hot assembly is combined with an array of lumped channels which represent the remaining assemblies within a core segment. Using this single geometry, boundary conditions are not required since the effect of the core is inherently included when computing the subchannel flows. Although single stage analyses have been performed previously (e.g., Reference 6), the thermal-hydraulic codes then in existence were capable of handling only a limited number of channels. This necessitated coarse simulations of the core consisting of only a few subchannels together

with very large lumped channels representing many assemblies. However, the recent development of the COBRA IIIC/MIT computer code[7] has provided the capability to analyze geometries consisting of up to 200 channels. Thus, it is now possible to perform single stage thermal analyses using the same radial nodalization as used in the traditional multistage analyses.

This concept has been applied by the Virginia Electric and Power Company (VEPCO) in the development of a core thermal-hydraulic analysis capability. This capability is based upon a single stage analysis which incorporates the geometries and methodologies used in multistage analyses. The accuracy of this approach has been verified through comparisons with analyses which were used in the design and licensing of the Surry Nuclear Power Station. Steady state and transient MDNBRs calculated using the VEPCO methods are in excellent agreement with those presented in the Surry Final Safety Analysis Report (FSAR)[8] and in subsequent licensing documents.[9,10,11,12]

The purpose of this report is to describe the VEPCO Thermal-Hydraulic Model and to present the comparisons which demonstrate the Model's accuracy. A discussion of the COBRA IIIC/MIT computer code is provided in Section 2. The hydraulic model of the Surry core and the corresponding thermal model are described respectively in Sections 3 and 4. Engineering uncertainties which were applied in the analyses are described in Section 5. Section 6 then describes the specific analyses which were performed and presents the comparisons of VEPCO results with those given in the licensing documents. Conclusions are provided in Section 7.

SECTION 2 - COBRA IIIC/MIT COMPUTER CODE DESCRIPTION

2.1 Introduction

The COBRA IIIC/MIT computer code[7], developed at the Massachusetts Institute of Technology for the Electric Power Research Institute, is a modified version of the more generally known COBRA IIIC computer code[13]. Both codes have the same basic organization, use the same conservation equations, and use essentially the same method of solution. COBRA IIIC/MIT will therefore yield essentially identical results to those of COBRA IIIC when applied to the same problem. However, the two distinguishing characteristics of COBRA IIIC/MIT compared with COBRA IIIC are its reduced computational running time and its ability to handle larger geometries. Thus, the COBRA IIIC/MIT code has the capability to more efficiently analyze detailed representations of PWR cores.

For these reasons, the COBRA IIIC/MIT computer code became the starting point in the development of the VEPCO Thermal-Hydraulic Model. In the course of this development, the original version was modified in order to correct several shortcomings and to provide additional user oriented flexibility. These modifications are summarized in Appendix A. A discussion of the code's method of solution is provided in Section 2.2. The code's empirical models and correlations that have been selected for use in the VEPCO Thermal-Hydraulic Model are described in Section 2.3. Computational input parameters are described in Section 2.4.

2.2 Method of Solution

The COBRA IIIC/MIT computer code calculates the flow and enthalpy within interconnected flow channels by solving finite difference equations

of continuity, energy, and momentum. The mathematical model is applicable to both steady state and transient conditions, and the model considers both turbulent mixing and diversion crossflow. In formulating the mathematical model, one-dimensional, two-phase, separated, slip-flow was assumed to exist during boiling. The two-phase flow structure was assumed to be fine enough to allow specification of void fraction as a function of enthalpy, flow rate, heat flux, pressure, position, and time. Sonic velocity propagation effects were not included. Within a channel, the diversion crossflow velocity was assumed to be small compared to the axial velocity. This assumption allowed the use of a simplified equation for the conservation of transverse momentum.

The equations are solved as a boundary value problem by using a semi-explicit finite difference scheme. The boundary conditions for the problem are the inlet enthalpy, inlet mass velocity, and exit pressure. The boundary value solution is obtained by assuming a uniform exit pressure distribution. (The equations do not require actual pressures since only pressure differences are used.) When performing a computation, the code iterates over the length of the core until convergence of the flow solution is obtained. Convergence is achieved when the change in any channel flow is less than a user specified fraction of the flow from the previous iteration.

The same finite difference equations are used for both steady state and transient computations. For steady state calculations, the time step, Δt, is set equal to an arbitrarily large value thereby negating the time dependent terms. For transient calculations, the time step is set equal to a user specified value. When performing a transient calculation, a steady state calculation is first performed to obtain initial conditions. Time dependent forcing functions consisting of inlet temperature, inlet flow, system pressure, and core average heat flux are used to establish boundary conditions at succeed-

ing times. The calculation iterates over the first time step until the flow solution converges. The converged solution is then used as the initial conditions for the new time, and the procedure continues for all of the subsequent time steps.

Although the equations of continuity, energy, and momentum form the basic structure of the mathematical model, their solution is still dependent upon the use of empirical correlations. Of major importance are the correlations used in calculating the pressure gradient and those used in calculating turbulent mixing. Once the flow solution is obtained, additional correlations are used in calculating the DNBR distribution. The COBRA IIIC/MIT computer code allows user specification of the appropriate correlations. The models and correlations which have been selected for use in the VEPCO Thermal-Hydraulic Model are described in the following subsection.

2.3 Models and Correlations

2.3.1 Void Fraction

Void fractions are predicted using the Smith void fraction correlation[14] in conjunction with the Levy subcooled void model.[15] The Levy model uses local heat flux and fluid conditions in predicting the true (non-equilibrium) quality. This true quality is then used in the Smith correlation to predict the void fraction in both the subcooled and bulk boiling regions.

2.3.2 Single and Two-Phase Friction Factors

In computing single and two-phase pressure drops, an isothermal friction factor correlation is used in conjunction with a wall viscosity correlation and a correlation for predicting two-phase friction multipliers. The isothermal friction factor, f_{ISO}, is calculated using the following correlation,[16]

$$f_{ISO} = 0.184(Re)^{-0.2}$$

where Re is the local Reynolds number. The isothermal friction factor is corrected for heating effects by the following relationship,[17]

$$\frac{f_H}{f_{ISO}} = 1.0 + \frac{\text{Heated Perimeter}}{\text{Wetted Perimeter}}\left[\left(\frac{\mu_{wall}}{\mu_{bulk}}\right)^{0.6} - 1.0\right]$$

where f_H is the heated friction factor, μ_{bulk} is the viscosity evaluated at the bulk fluid temperature, and μ_{wall} is the viscosity evaluated at the wall temperature. The wall temperature, T_{wall}, is calculated using the following relationship,

$$T_{wall} = T_{bulk} + \frac{q''}{h}$$

where q'' is the surface heat flux and T_{bulk} is the bulk fluid temperature. The heat transfer coefficient, h, is calculated from the Dittus-Boelter correlation[18] using bulk fluid properties. In the two-phase flow region, the Baroczy correlation[19] is used to calculate two-phase friction multipliers which are applied to the heated friction factor.

2.3.3 Turbulent Mixing

The degree of turbulent mixing between adjacent channels is calculated using the following relationship,

$$w' = \beta s \bar{G}$$

where w' is the turbulent transverse fluctuating flow rate per axial length, $\bar{G}$ is the average mass velocity of the adjacent channels, s is the common gap, and β is the mixing coefficient. The above relationship is used to predict both single and two-phase mixing.

2.3.4 Critical Heat Flux Correlation

In predicting the non-uniform critical heat flux, the W-3 correlation[20] is used in conjunction with the F-factor correlation.[20] In determining the lower bound of the F-factor integral, the Jens and Lottes correlation[21] is used to predict the axial position where nucleate boiling begins. When appropriate, the coldwall factor[20] and the L-grid or R-grid spacer factor[22] are used with the W-3 correlation to predict the critical heat flux. (If required, other CHF correlations can be easily added to the code as options.)

2.3.5 Water Properties

Water properties (enthalpy, specific volume, viscosity, conductivity, and specific heat) are calculated using the HOH routines which were obtained from Reference 23.

2.4 Computational Input Parameters

The computational input parameters that were used in the Surry analyses described within this report are listed in Table 2-1. For steady state analyses, 156 axial intervals were specified (1" intervals), and for transient analyses, 78 axial intervals were specified (2" intervals). Values chosen for the crossflow resistance coefficient, the mixing coefficient, and the momentum factors are representative of those which would be used in subchannel analyses.[13]

TABLE 2-1

COMPUTATIONAL INPUT PARAMETERS

Number of Axial Intervals, Steady State Analysis	156
Number of Axial Intervals, Transient Analysis	78
Fraction of Heat Generated in the Fuel	0.974
Convergence Criteria	0.005
Crossflow Resistance Coefficient, k	0.5
Mixing Coefficient, β	0.019
Turbulent Momentum Factor, f_t	0.0
Transverse Momentum Factor, s/ℓ	0.5

SECTION 3 - HYDRAULIC MODEL DESCRIPTION

3.1 Introduction

The techniques used in formulating the hydraulic representation of the Surry core are applicable, in general, to all pressurized water reactors. (These same techniques will be used in formulating the hydraulic models for the North Anna cores.) Basically, eighth core symmetry is assumed, and thus only a 1/8 core segment is modeled. It is also assumed that the hot assembly is located at the center of the core, and therefore, due to symmetry the 1/8 core segment contains 1/8 of the hot assembly. The hot assembly is modeled as an array of subchannels, while the remaining assemblies are modeled as an array of lumped channels. For steady state analysis, a fine mesh geometry is used in which each lumped assembly and each hot assembly subchannel are modeled as individual flow channels. For transient analysis, a coarse mesh geometry is used in which assemblies and subchannels are combined to form larger channels. Because the coarser geometry contains fewer channels, less computational time per iteration is required, allowing the transient analysis to be performed without excessive expeditures of computer time.

Using the above mentioned general techniques, hydraulic models have been developed at VEPCO which are applicable specifically to the Surry units. A 53 channel model has been developed for steady state analysis, and using this model as a basis, a 19 channel model has been developed for transient analysis. Detailed descriptions of these models along with a general description of the Surry core are provided in the following subsections.

3.2 General Description of the Surry Core

The Surry Units No. 1 and 2 are Westinghouse designed pressurized water reactors with cores consisting of 157 fuel assemblies. The arrangement

of the fuel assemblies is shown in Figure 3-1. Each fuel assembly is hydraulically identical and consists of 204 fuel rods, 20 guide thimble tubes, and a centrally located instrumentation tube. As shown in Figure 3-2, the fuel assembly elements are arranged in a 15 x 15 square array. Assembly hydraulic parameters are listed in Table 3-1.

Seven grids are used in each fuel assembly to support the fuel rods. Each grid consists of individual slotted straps interlocked and brazed in an "egg-crate" arrangement. The grids maintain the lateral spacings between fuel rods, and they are located at intervals along the assembly length. The five middle grids are called mixing vane grids since they contain tabs which project into the coolant stream. These grids are used in the high heat flux region to promote better mixing of the coolant. The internal straps of the two end grids do not contain mixing vanes, and they are therefore called non-mixing vane grids. All seven grids are mechanically attached to the guide thimble tubes. The guide thimble tubes are in turn attached to the upper and lower nozzles and thus provide assembly structural support. A side view of the Westinghouse 15 x 15 assembly is shown in Figure 3-3.

3.3 Eighth Core Representation - 53 Channel Model

In modeling the Surry core for steady state analysis, a 53 channel model was developed representing a 1/8 core segment. This 53 channel model consisted of 25 lumped assembly channels and 28 subchannels. The assembly radial geometry is shown in Figure 3-4, and the subchannel radial geometry is shown in Figure 3-5. In the axial direction, the seven grids were modeled by using grid loss coefficients at the axial positions listed in Table 3-2. The upper and lower nozzles had been initially modeled, however, they were subsequently deleted after it was found that they had only a minor effect on the flow solution.

Within the assembly geometry, each lumped assembly was modeled by using a lumped flow area, lumped heated and wetted perimeters, and an effective gap. These hydraulic data, listed in Table 3-3, were calculated by considering the individual elements comprising the fuel assembly. The effective gap for crossflow was calculated by subtracting from the assembly pitch the blockage caused by a row of fuel rods (i.e., 15 x fuel rod diameter). Half assemblies, formed by the lines of symmetry, were modeled by multiplying the assembly hydraulic data by 0.5.

Within the subchannel geometry, four different types of subchannels were modeled. As shown in Figure 3-5, these subchannel types consist of a unit cell, a perimeter cell, a corner cell, and a thimble cell. The unit, perimeter, and corner cells are all flow channels which are basically formed by four fuel rods. However, the perimeter and corner cells are modeled to include the flow region between the fuel rods of adjacent assemblies. The fourth type of subchannel is the thimble cell which is formed by three fuel rods and a guide/instrumentation thimble tube. All the subchannels were modeled using the hydraulic data shown in Tables 3-4 through 3-7.

3.4 Eighth Core Representation - 19 Channel Model

In modeling the Surry core for transient analysis, a 19 channel model was developed to represent the 1/8 core segment. This model was derived from the 53 channel model by combining assemblies and subchannels to form larger, lumped channels. As shown in Figures 3-6 and 3-7, the 19 channel model consists of 4 lumped channels and 15 subchannels. The lumped channels were modeled using the hydraulic data shown in Table 3-8. The subchannels were modeled using the data provided in Tables 3-4 and 3-7.

TABLE 3-1

ASSEMBLY HYDRAULIC PARAMETERS

No. of Fuel Rods	204
No. of Guide Thimble Tubes	20
No. of Instrumentation Thimble Tubes	1
Fuel Rod Outside Diameter (inches)	0.422
Guide Thimble Tube Outside Diameter (inches)	0.546
Instrumentation Thimble Tube Outside Diameter (inches)	0.546
Fuel Rod Pitch (inches)	0.563
Fuel Assembly Pitch (inches)	8.466

TABLE 3-2

AXIAL POSITIONS OF ASSEMBLY COMPONENTS

Description	Position (inches)
Start of Assembly	0.00
Start of Rodded Region	2.30
Start of Active Fuel	3.00
Non-mixing Vane Grid	4.42
Mixing Vane Grid	28.62
Mixing Vane Grid	54.81
Mixing Vane Grid	81.00
Mixing Vane Grid	107.19
Mixing Vane Grid	133.38
End of Active Fuel*	146.60
Non-mixing Vane Grid	152.06
End of Rodded Region	154.10
End of Assembly	156.00

* Based upon an active fuel length of 143.60 inches

TABLE 3-3 ASSEMBLY HYDRAULIC DATA

Fuel Assembly Flow Area (square inches)	38.22
Fuel Assembly Wetted Perimeter (inches)	306.5
Fuel Assembly Heated Perimeter (inches)	270.5
Fuel Assembly Effective Gap (inches)	2.136
Fuel Assembly Non-mixing Vane Grid Loss Coefficient	0.7378
Fuel Assembly Mixing Vane Grid Loss Coefficient	0.9182

TABLE 3-4 UNIT CELL HYDRAULIC DATA

Unit Cell Flow Area (square inches)	0.1771
Unit Cell Wetted Perimeter (inches)	1.326
Unit Cell Heated Perimeter (inches)	1.326
Fuel Rod to Fuel Rod Gap (inches)	0.141
Unit Cell Non-mixing Vane Grid Loss Coefficient	0.6732
Unit Cell Mixing Vane Grid Loss Coefficient	0.8377

TABLE 3-5 PERIMETER CELL HYDRAULIC DATA

Perimeter Cell Flow Area (square inches)	0.2716
Perimeter Cell Wetted Perimeter (inches)	1.989
Perimeter Cell Heated Perimeter (inches)	1.989
Fuel Rod to Fuel Rod Gap (inches)	0.141
Perimeter Cell Non-mixing Vane Grid Loss Coefficient	0.6732
Perimeter Cell Mixing Vane Grid Loss Coefficient	0.8377

TABLE 3-6 CORNER CELL HYDRAULIC DATA

Corner Cell Flow Area (square inches)	0.4163
Corner Cell Wetted Perimeter (inches)	2.983
Corner Cell Heated Perimeter (inches)	2.983
Fuel Rod to Fuel Rod Gap (inches)	0.141, 0.222
Corner Cell Non-mixing Vane Grid Loss Coefficient	0.6732
Corner Cell Mixing Vane Grid Loss Coefficient	0.8377

TABLE 3-7 THIMBLE CELL HYDRAULIC DATA

Thimble Cell Flow Area (square inches)	0.1535
Thimble Cell Wetted Perimeter (inches)	1.423
Thimble Cell Heated Perimeter (inches)	0.994
Fuel Rod to Fuel Rod Gap (inches)	0.141
Fuel Rod to Guide Thimble Tube Gap (inches)	0.079
Thimble Cell Non-mixing Vane Grid Loss Coefficient	0.8953
Thimble Cell Mixing Vane Grid Loss Coefficient	1.114

TABLE 3-8 HYDRAULIC DATA FOR LUMPED CHANNELS

Channel No. 1	
Flow Area (square inches)	57.33
Wetted Perimeter (inches)	459.75
Heated Perimeter (inches)	405.75
Effective Gap (inches)	3.204
Non-mixing Vane Grid Loss Coefficient	0.7378
Mixing Vane Grid Loss Coefficient	0.9182
Channel No. 2	
Flow Area (square inches)	649.74
Wetted Perimeter (inches)	5210.5
Heated Perimeter (inches)	4598.5
Effective Gap (inches)	3.204
Non-mixing Vane Grid Loss Coefficient	0.7378
Mixing Vane Grid Loss Coefficient	0.9182
Channel No. 3	
Flow Area (square inches)	38.22
Wetted Perimeter (inches)	306.5
Heated Perimeter (inches)	270.5
Effective Gap (inches)	3.204, 1.068
Non-mixing Vane Grid Loss Coefficient	0.7378
Mixing Vane Grid Loss Coefficient	0.9182

TABLE 3-8 HYDRAULIC DATA FOR LUMPED CHANNELS (Continued)

Channel No. 4

Flow Area (square inches)	2.729
Wetted Perimeter (inches)	21.06
Heated Perimeter (inches)	19.55
Effective Gap (inches)	1.068
Non-mixing Vane Grid Loss Coefficient	0.7099
Mixing Vane Grid Loss Coefficient	0.8833

FIGURE 3-1

FUEL ASSEMBLY ARRANGEMENT OF SURRY CORE

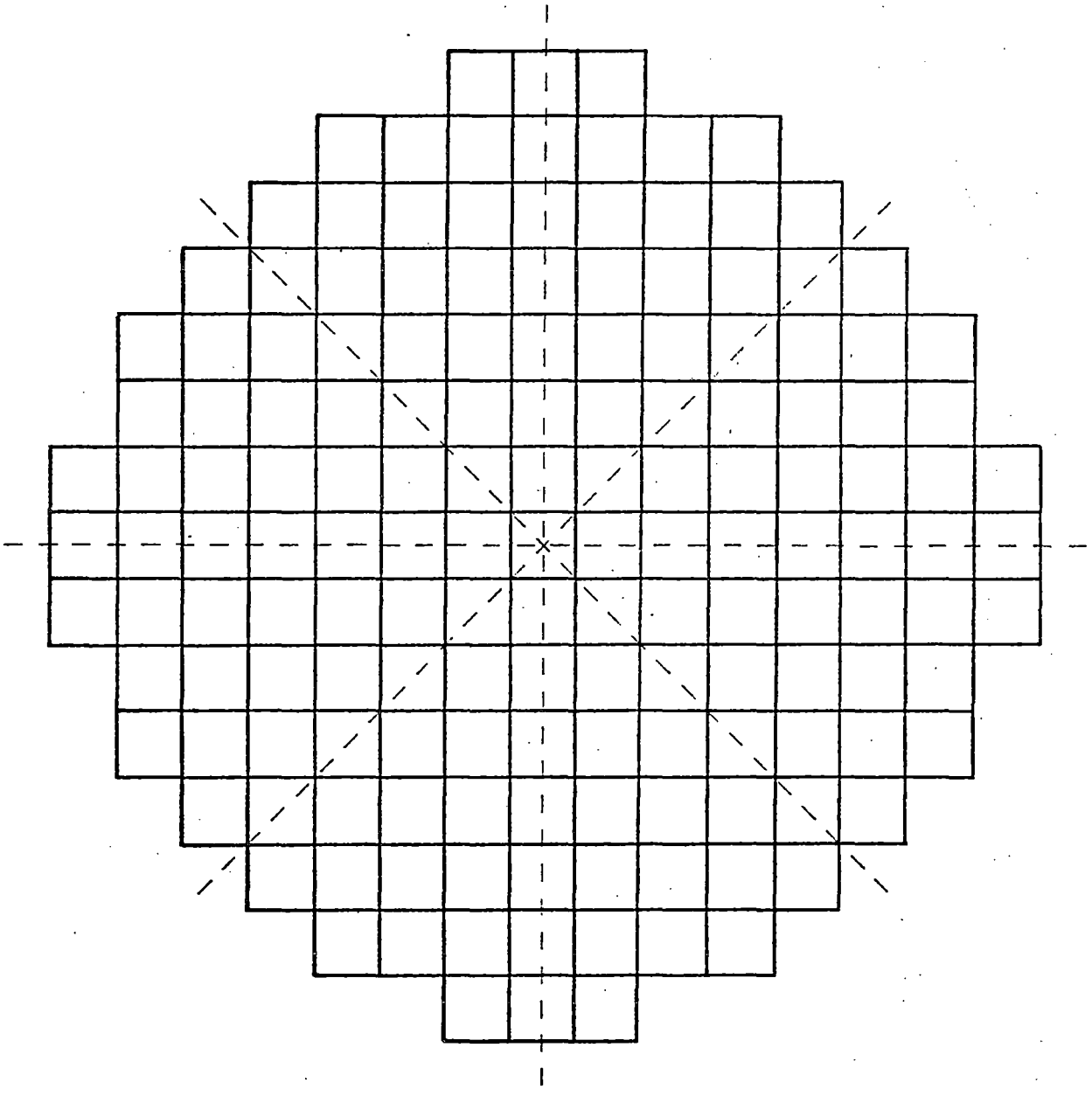

FIGURE 3-2

CROSS SECTIONAL VIEW OF SURRY FUEL ASSEMBLY

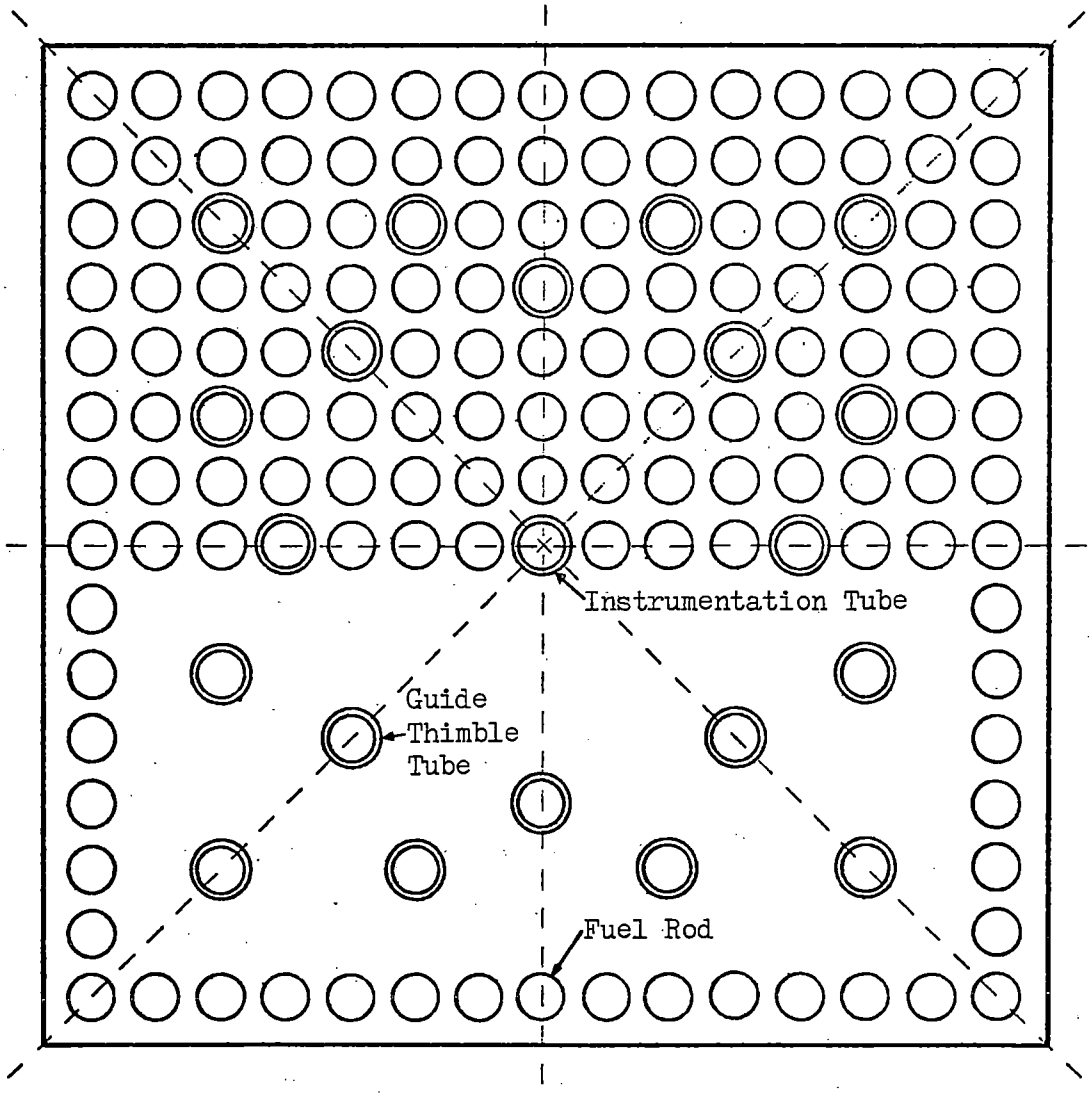

FIGURE 3-3

SIDE VIEW OF SURRY FUEL ASSEMBLY

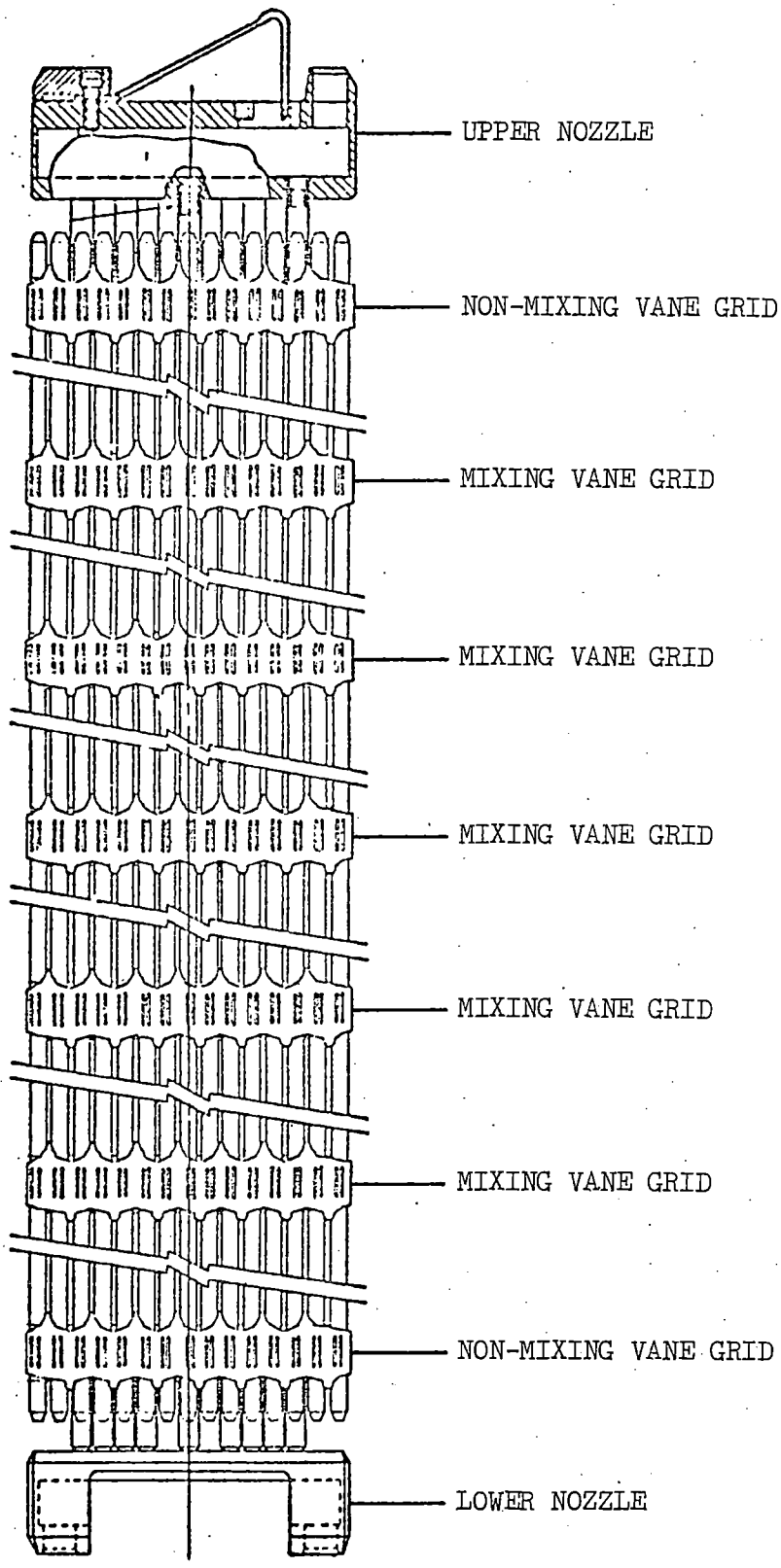

FIGURE 3-4

ASSEMBLY GEOMETRY OF 53 CHANNEL MODEL

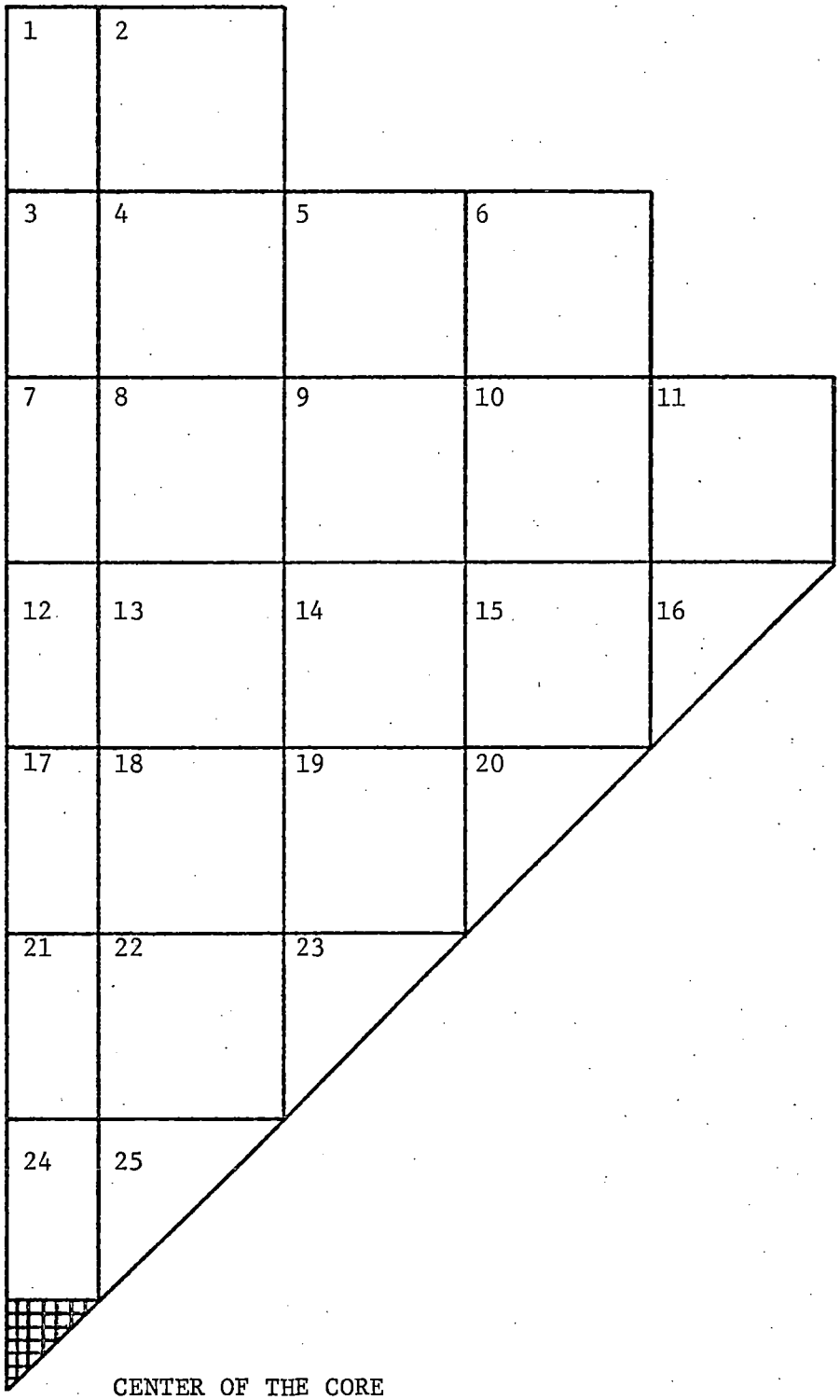

FIGURE 3-5

SUBCHANNEL GEOMETRY OF 53 CHANNEL MODEL

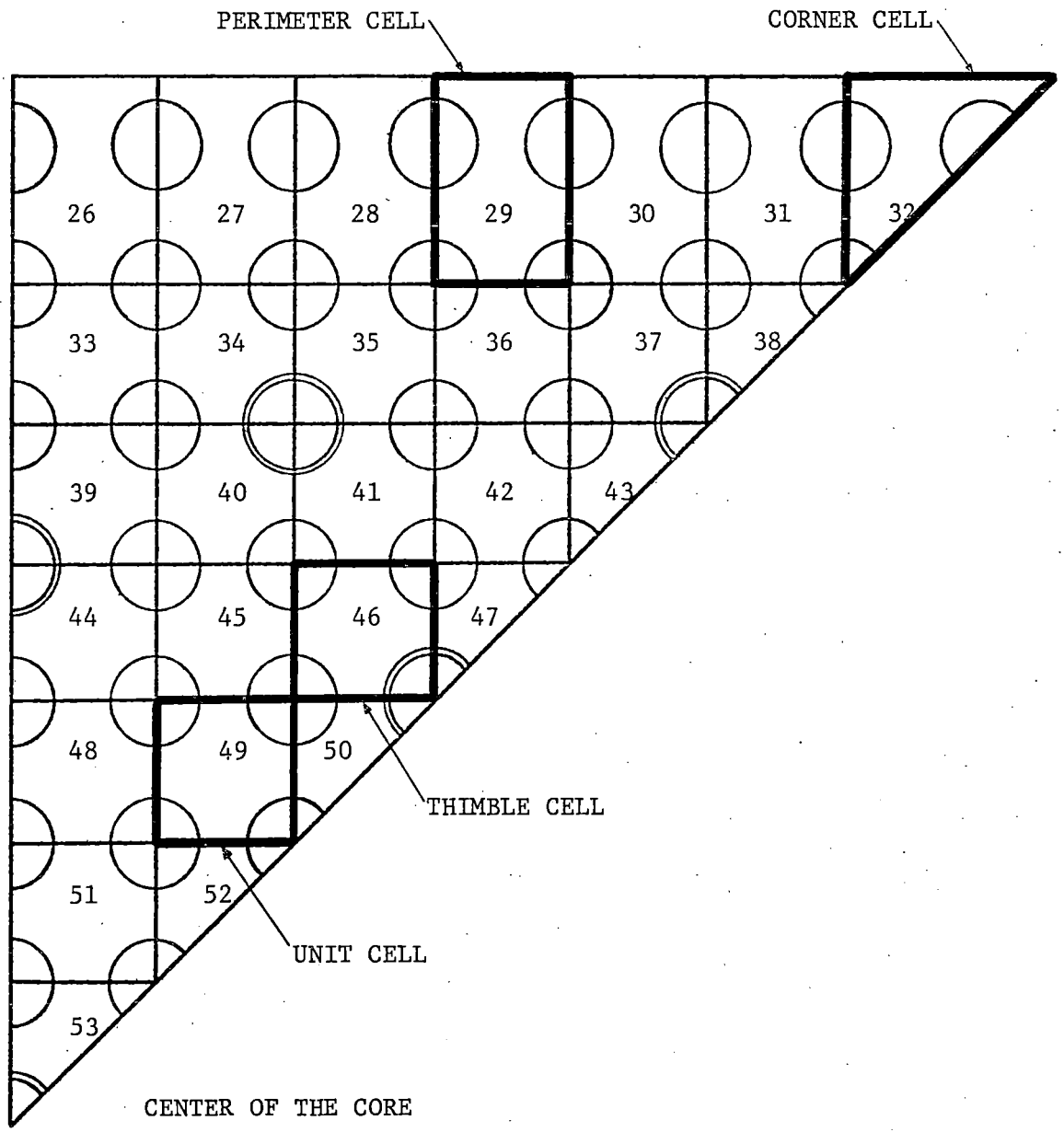

FIGURE 3-6

ASSEMBLY GEOMETRY OF 19 CHANNEL MODEL

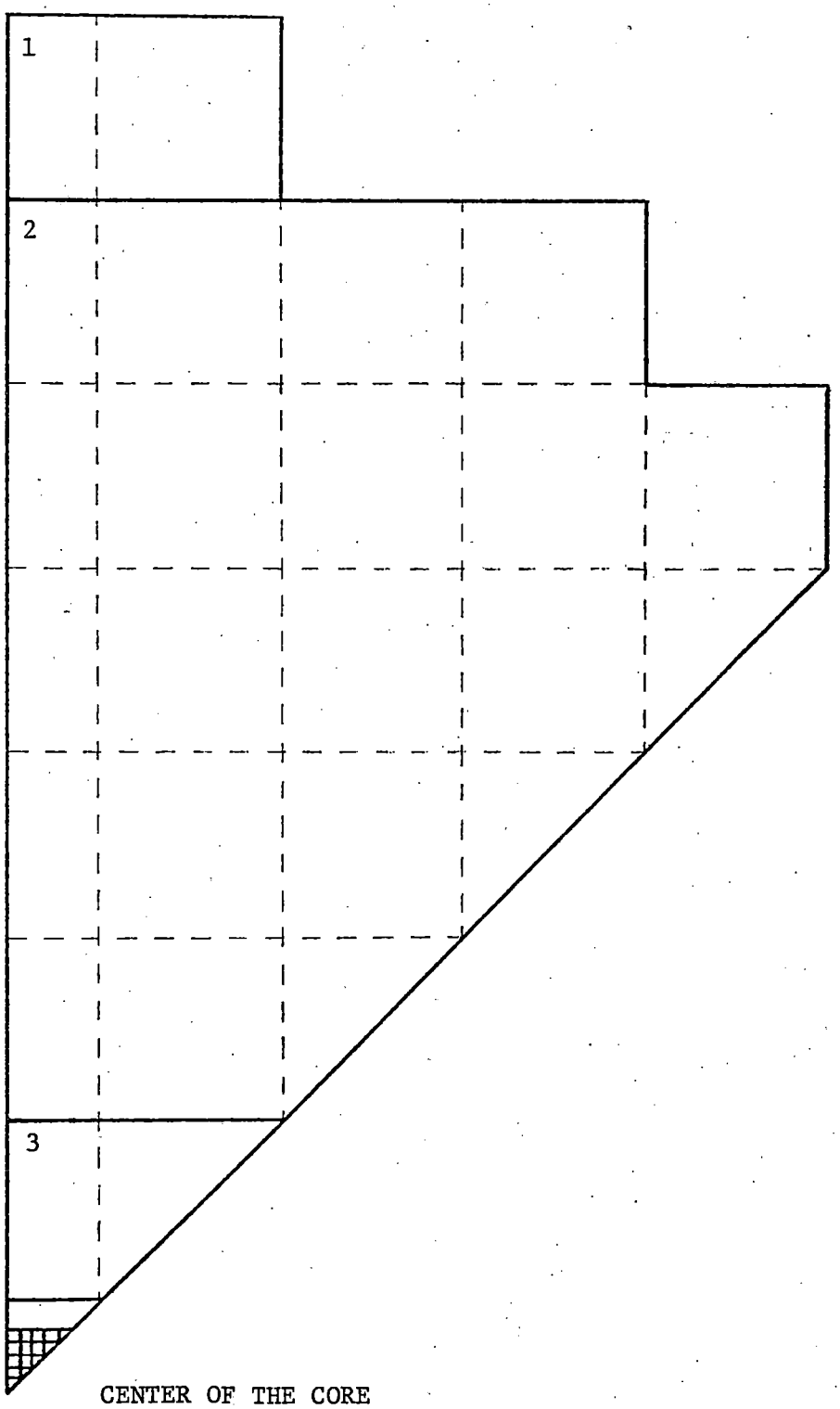

FIGURE 3-7

SUBCHANNEL GEOMETRY OF 19 CHANNEL MODEL

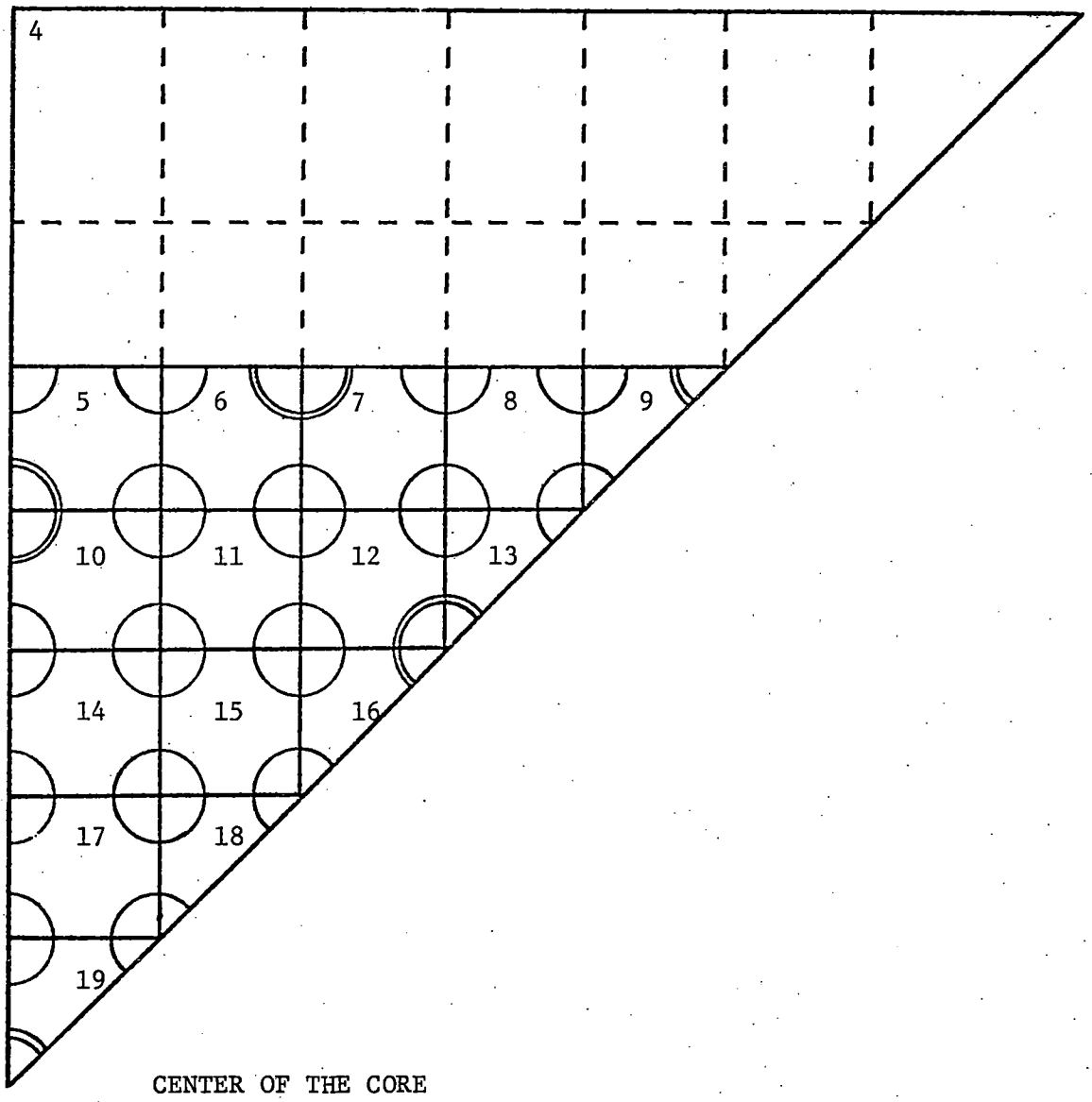

SECTION 4 - THERMAL MODEL DESCRIPTION

4.1 Introduction

The techniques used in formulating the thermal representation of the Surry core are applicable, in general, to all pressurized water reactors. (The same techniques will be used in formulating the thermal models for the North Anna cores.) The thermal model basically consists of an inlet flow distribution, radial and axial power distributions, and appropriate reactor operating conditions. For transient analysis, time dependent forcing functions of system pressure, inlet flow, inlet temperature, and core average heat flux are also specified.

Thermal-hydraulic design parameters form the basis of the model. Thus, the radial power distribution is based upon the design value of $F^N_{\Delta H}$, and the axial power distribution is based upon the reference axial flux shape. The thermal design flow rate is used in determining the core average mass velocity, and thermal-hydraulic design values for inlet temperature, system pressure, and power level are used as operating conditions.

In formulating the inlet flow distribution, the inlet flow to the hot assembly (i.e., the subchannel array) is conservatively reduced by 5% in order to account for the possibility of inlet flow maldistribution. In order to conserve the total core flow rate, the peripheral assemblies are given inlet flow fractions slightly greater than 1.0. The average of all the flow fractions is forced to equal 1.0.

In formulating the subchannel portion of the radial power distribution, the fuel rods which form the hot channel are given relative powers equal to the design value of $F^N_{\Delta H}$. Lower relative powers for the remaining fuel rods are then assigned to create a gradual power gradient which peaks around the hot channel. The average of all the fuel rod relative powers is forced to

equal the hot assembly relative power. (In general, power peaking within the hot assembly is assumed to be 5%, i.e., the ratio of $F^N_{\Delta H}$ and the hot assembly relative power is 1.05.)

In formulating the assembly portion of the radial power distribution, the hot assembly relative power is also assigned to the two assemblies which are adjacent to the subchannel array. Lower relative powers for the remaining assemblies are then assigned to create a second power gradient which peaks around the hot assembly. The average of all the assembly relative powers is forced to equal 1.0.

The above mentioned general techniques are used to formulate the overall thermal model. The thermal model is then imposed upon the hydraulic model in order to obtain the complete thermal-hydraulic representation of the core. Since this representation is dependent upon thermal-hydraulic design parameters, revised representations must be considered in the event of any subsequent design changes. In general, the hydraulic model remains relatively fixed since it is affected only by changes in the mechanical design of the fuel. However, the thermal model can be significantly affected by changing any one of the previously mentioned design parameters. Two such changes have occurred since the original design of the Surry units. These design changes are discussed in Section 4.2. Sections 4.3 through 4.6 then describe the thermal model which has been formulated based upon current Surry design parameters. (The thermal models which are based upon earlier designs are described in detail in Section 6.)

4.2 General Description of the Thermal-Hydraulic Design of the Surry Core

The Surry Units No. 1 and 2 are Westinghouse designed, three loop pressurized water reactors with thermal ratings of 2441 MWt[8]. The thermal design flow rate is 265,500 gpm which is based upon three reactor coolant

pumps each rated at a design capacity of 88,500 gpm at 543 °F. The assumed fraction of flow effective for heat removal from the core is 0.955 (i.e., 4.5% core bypass). The nominal inlet temperature is 543 °F, and the nominal operating pressure is 2250 psia. The fuel rods have a nominal active length of 144.0", and the fraction of heat generated in the fuel is 0.974. In the original design of the Surry units, $F^N_{\Delta H}$ was 1.58, and a chopped cosine with a 1.72 peak was used as the reference axial power distribution.

Several revisions to the above parameters have been required since the publication of the original FSAR. In December, 1972, the design peaking factors were revised in the densification reanalysis.(9) $F^N_{\Delta H}$ was reduced from 1.58 to 1.55, and the reference axial power distribution for DNB analysis was changed to a chopped cosine with a 1.55 peak. Due to the phenomenon of fuel densification, the active length was reduced from 144.0 inches to 142.3 inches.

In August, 1977, the thermal design flow rate was reduced to 238,950 gpm at 543 °F which is 90% of the original thermal design flow rate.(12) This reduction in flow was a result of conservative assumptions concerning increased flow resistance associated with a limiting steam generator tube plugging level. Based upon revised fuel parameters, the active length of the fuel was assumed to be 143.6 inches.

4.3 Inlet Flow Distribution

The inlet flow distribution used with the 53 channel model is shown in Figure 4-1, and the inlet flow distribution used with the 19 channel model is shown in Figure 4-2. These distributions were used in all the DNB analyses described within this report. As shown in the figures, the hot assembly (i.e., the subchannel array) is given an inlet flow fraction of 0.95, while the peripheral assemblies are given flow fractions slightly greater than 1.0. The average of all the flow fractions is approximately equal to 1.0.

4.4 Power Distribution

The design radial power distribution which has been formulated by VEPCO for the current thermal model is shown in Figures 4-3 through 4-6. (Since this thermal model is based upon the reduced thermal design flow rate,[12] it is referred to as the Low Flow Assumption Reanalysis.) Figure 4-3 shows the assembly power distribution which is applicable to the 53 channel model. As shown, a power gradient exists which peaks around the hot assembly located at the center of the core. The hot assembly as well as the adjacent assemblies are given relative powers of 1.475, while lower relative powers are assigned to the remaining assemblies. The average of all the assembly relative powers is 1.0. The assembly power distribution for the 19 channel model is derived from that of the 53 channel model by averaging all but the three central assembly relative powers. Figure 4-4 shows the resulting assembly power distribution used with the 19 channel model.

Figure 4-5 shows the subchannel portion of the radial power distribution applicable to the 53 channel model. Within the subchannel array, a second power gradient exists, and it peaks around the hot channel which is a thimble cell. As shown in Figure 4-5, the three fuel rods surrounding the hot thimble cell are each given relative powers of 1.55, while lower relative powers are assigned to the remaining fuel rods. The average of all the fuel rod relative powers is equal to the hot assembly relative power, or 1.475. The subchannel power distribution for the 19 channel model is derived from that of the 53 channel model by averaging the relative powers of the fuel rods located within the lumped subchannel. Figure 4-6 shows the resulting subchannel power distribution used with the 19 channel model.

The same axial power distribution is used in both the 19 and 53 channel models. For the current thermal model, the reference axial flux

shape is a 1.55 chopped cosine which is based upon an active length of 143.6 inches. Values of relative flux as a function of axial position are obtained by using the following equation,

$$F(z') = 1.55 \cos \frac{\pi z'}{H_e}$$

where $F(z')$ = relative axial flux

z' = distance from the core center, feet

H_e = extrapolated length, feet

In determining the extrapolated length, H_e, the integral of the above equation is averaged over the active length and set equal to 1.0. An iterative process is then used in order to determine the value of H_e which satisfies the resulting equation. Table 4-1 lists axial flux values which define the axial power distribution used in the current thermal model.

4.5 Reactor Operating Conditions

Reactor conditions consist of a power level, a core flow rate, a core inlet temperature, and a system pressure. As previously discussed in Section 4.2, the Surry units are rated at 2441 MWt, the reactor thermal design flow rate is currently 238,950 gpm, the nominal inlet temperature is 543 ^{o}F, and the nominal system pressure is 2250 psia. When performing transient analysis, maximum steady state instrumentation errors are applied to these rated values so that the initial reactor conditions obtained are the most adverse with respect to thermal margin to DNB. This is accomplished by increasing the power by 2% to 2490 MWt, by increasing the temperature by 4 ^{o}F to 547 ^{o}F, and by decreasing the pressure by 30 psi to 2220 psia.

The power level is input as a core average heat flux which is calculated using the following equation,

$$Q'' = \frac{(FRAC)(POWER)}{(HP)(ACTIVE\ LENGTH)} \times \left(\frac{3413 \times 10^3\ Btu/hr}{MW}\right)$$

where Q'' = core average heat flux, $Btu/hr\text{-}ft^2$

FRAC = fraction of rated power

POWER = nominal thermal power, MW

HP = total core heated perimeter, feet

ACTIVE LENGTH = core active length, feet

The core average heat flux is based upon the total heat generation rate because it is used within the COBRA IIIC/MIT code to determine the total heat added to the coolant. Modifications have been added to the code by VEPCO in order to account for the fraction of the heat which is actually generated within the fuel (See Appendix A).

The core flow rate is input to the COBRA IIIC/MIT code as a core average mass velocity. The core average mass velocity is calculated using the following equation,

$$G = \frac{(FRAC)(Q)(\rho)}{(FLOW\ AREA)} \times \left(\frac{60\ min}{hr}\right) \times \left(\frac{1\ ft^3}{7.4805\ gal}\right)$$

where G = core average mass velocity, $lbm/hr\text{-}ft^2$

FRAC = fraction of reactor flow effective for heat removal from the core (i.e., 0.955)

Q = reactor volumetric flow rate, gpm

ρ = fluid density at inlet, lbm/ft^3

FLOW AREA = total core flow area, ft^2

4.6 Forcing Functions for Transient Analysis

When performing a transient analysis, forcing functions are applied to the initial reactor conditions in order to obtain subsequent reactor conditions. For each reactor parameter that is changing with time, a forcing function is input as a table set with each entry consisting of the ratio of the transient condition to the initial condition and a corresponding time. The COBRA IIIC/MIT computer code has the capability of handling four different forcing functions, e.g., core average heat flux versus time, inlet flow versus time, inlet temperature versus time, and system pressure versus time.

For the Surry transient analyses described within this report, the forcing functions were obtained from the FSAR and other licensing documents. It has also been demonstrated that the forcing functions can be obtained from transient analyses performed using a system thermal-hydraulic code such as RETRAN.[24]

TABLE 4-1

AXIAL POWER DISTRIBUTION
(LOW FLOW ASSUMPTION REANALYSIS)

$$F(z') = 1.55 \cos\left(\frac{\pi z'}{12.12993429}\right)$$

Axial Flux Shape: 1.55 Cosine (143.6" Active Length)

z Axial Position (inches)	z' Fuel Position (feet)	z/156.0 Relative Position	F(z') Relative Flux
0.0	-	0.0000	0.0000
2.96	-	0.0190	0.0000
3.0	-5.98333333	0.0192	0.0328
10.0	-5.4	0.0641	0.2656
17.2	-4.8	0.1103	0.4988
24.4	-4.2	0.1564	0.7199
31.6	-3.6	0.2026	0.9237
38.8	-3.0	0.2487	1.1052
46.0	-2.4	0.2949	1.2601
53.2	-1.8	0.3410	1.3846
60.4	-1.2	0.3872	1.4757
67.6	-0.6	0.4333	1.5313
74.8	0.0	0.4795	1.5500
82.0	0.6	0.5256	1.5313
89.2	1.2	0.5718	1.4757
96.4	1.8	0.6179	1.3846
103.6	2.4	0.6641	1.2601
110.8	3.0	0.7103	1.1052
118.0	3.6	0.7564	0.9237
125.2	4.2	0.8026	0.7199
132.4	4.8	0.8487	0.4988
139.6	5.4	0.8949	0.2656
146.6	5.98333333	0.9397	0.0328
146.64	-	0.9400	0.0000
156.0	-	1.0000	0.0000

FIGURE 4-1

INLET FLOW DISTRIBUTION OF 53 CHANNEL MODEL

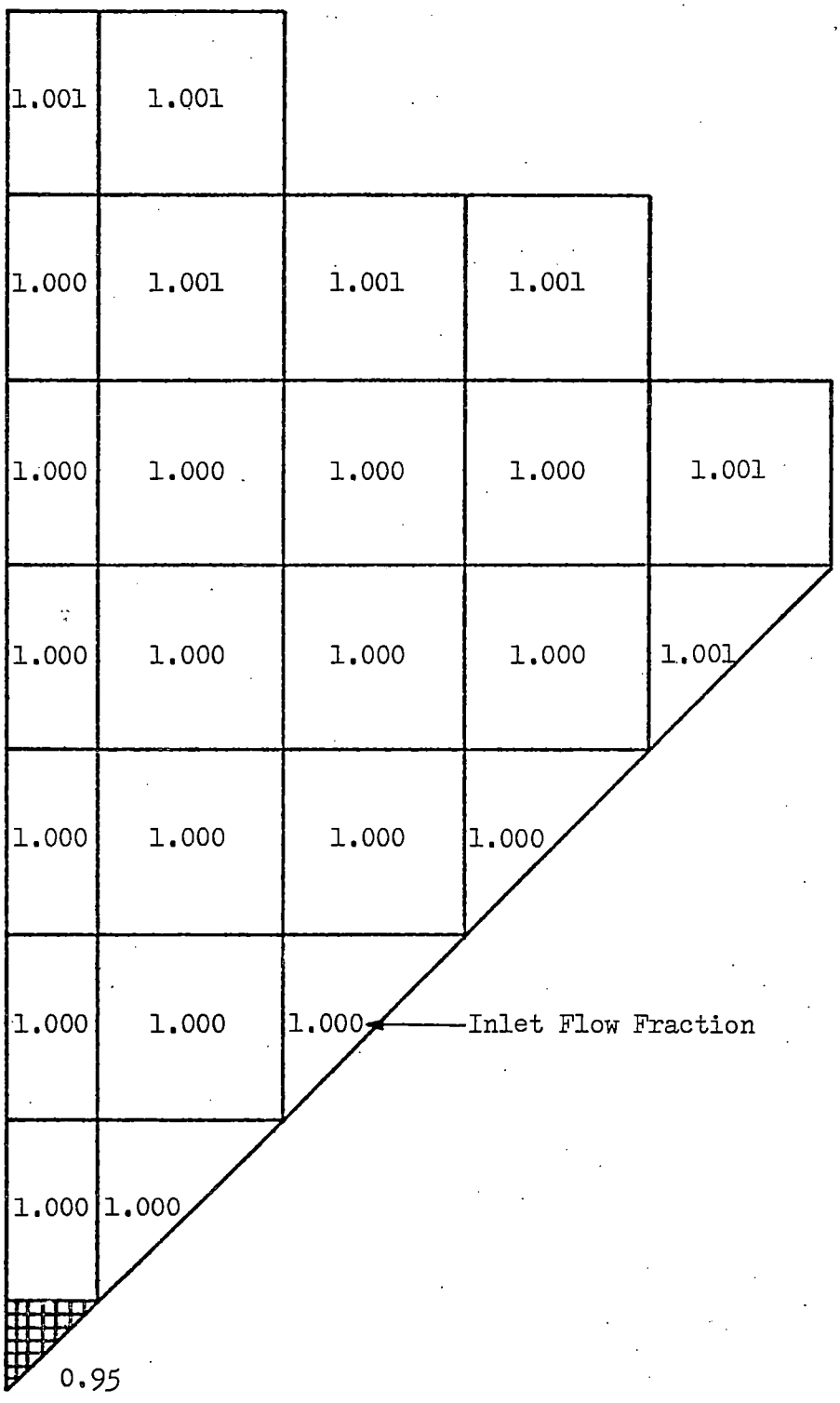

FIGURE 4-2

INLET FLOW DISTRIBUTION OF 19 CHANNEL MODEL

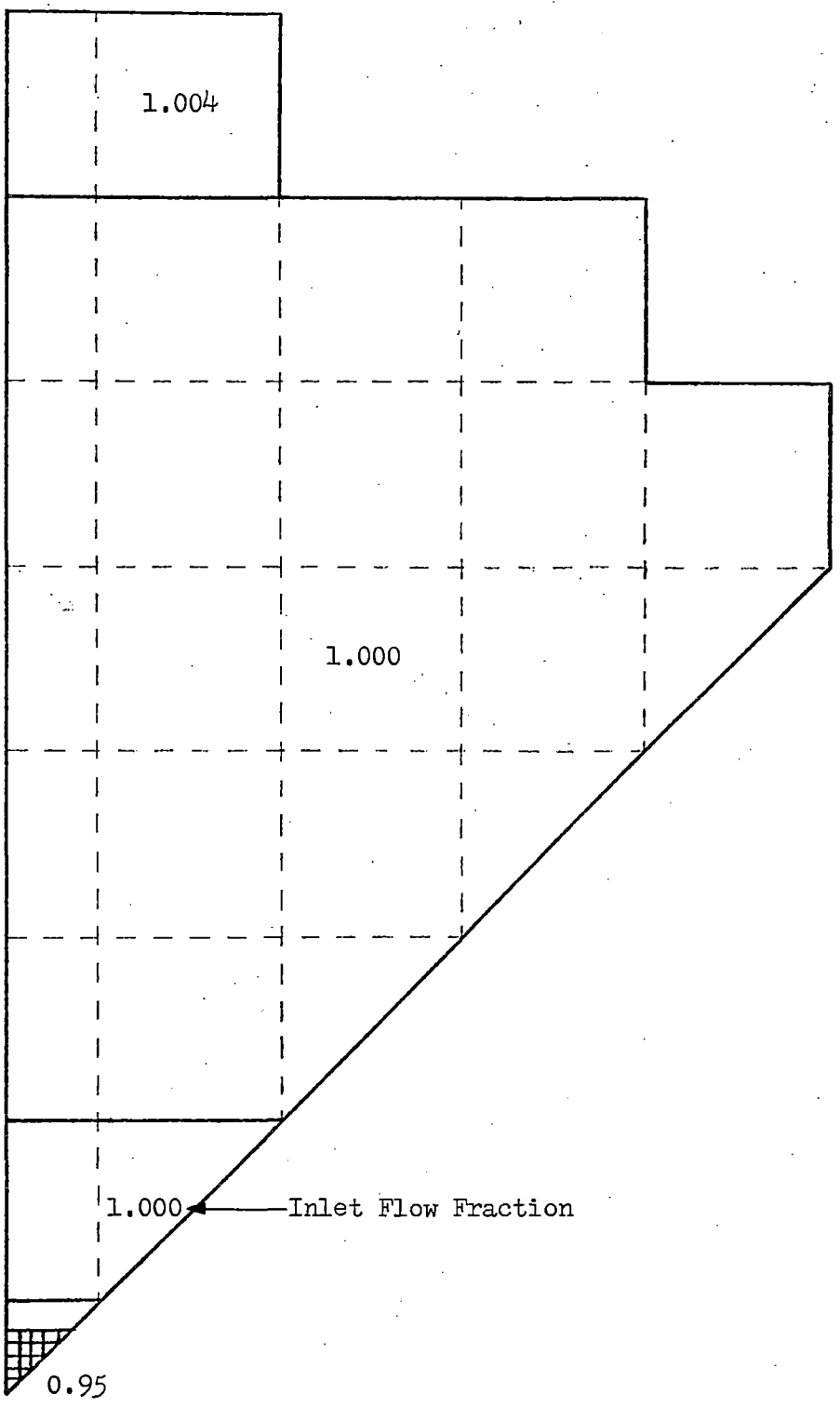

FIGURE 4-3

ASSEMBLY POWER DISTRIBUTION, 53 CHANNEL MODEL
(LOW FLOW ASSUMPTION REANALYSIS)

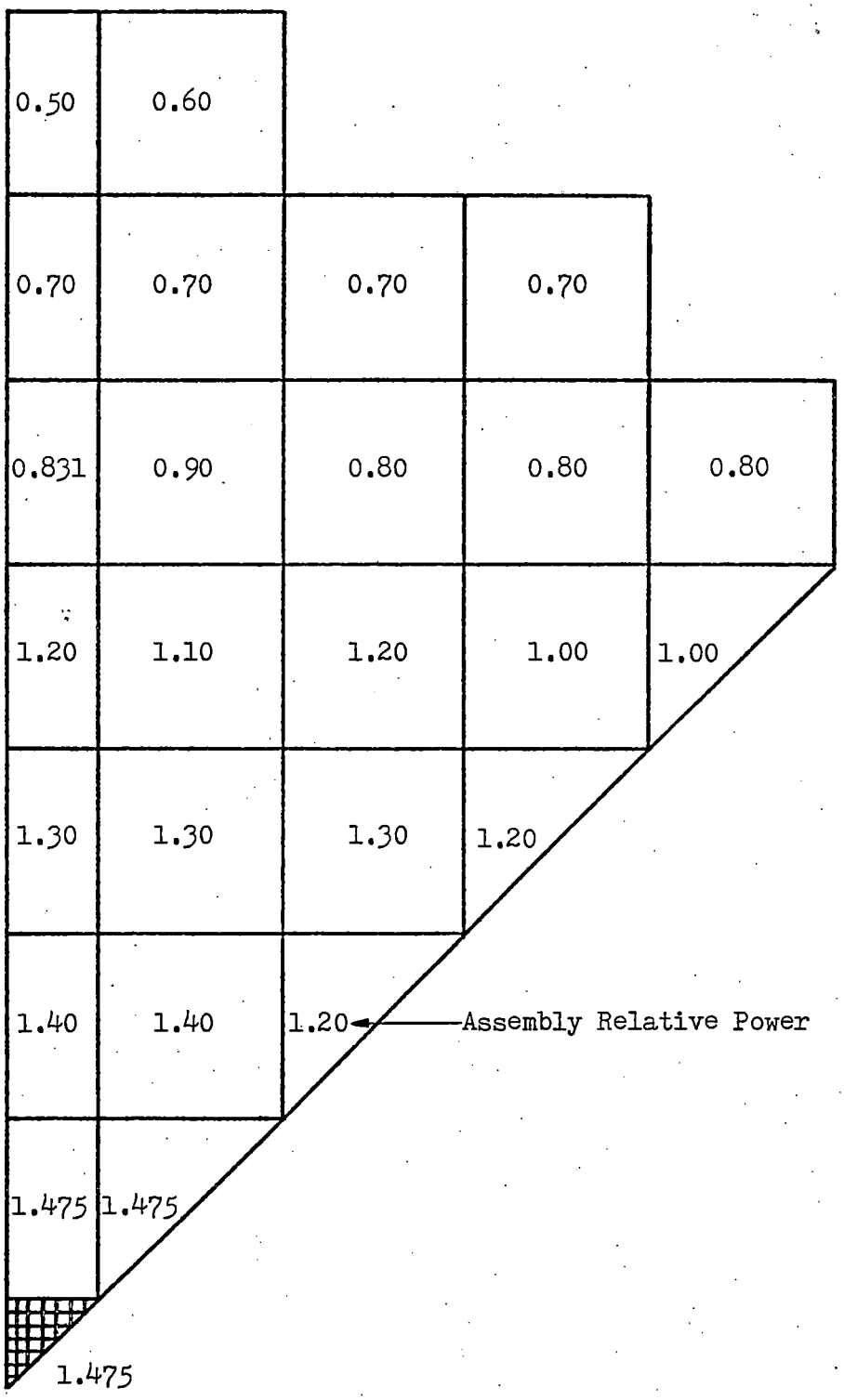

FIGURE 4-4

ASSEMBLY POWER DISTRIBUTION, 19 CHANNEL MODEL
(LOW FLOW ASSUMPTION REANALYSIS)

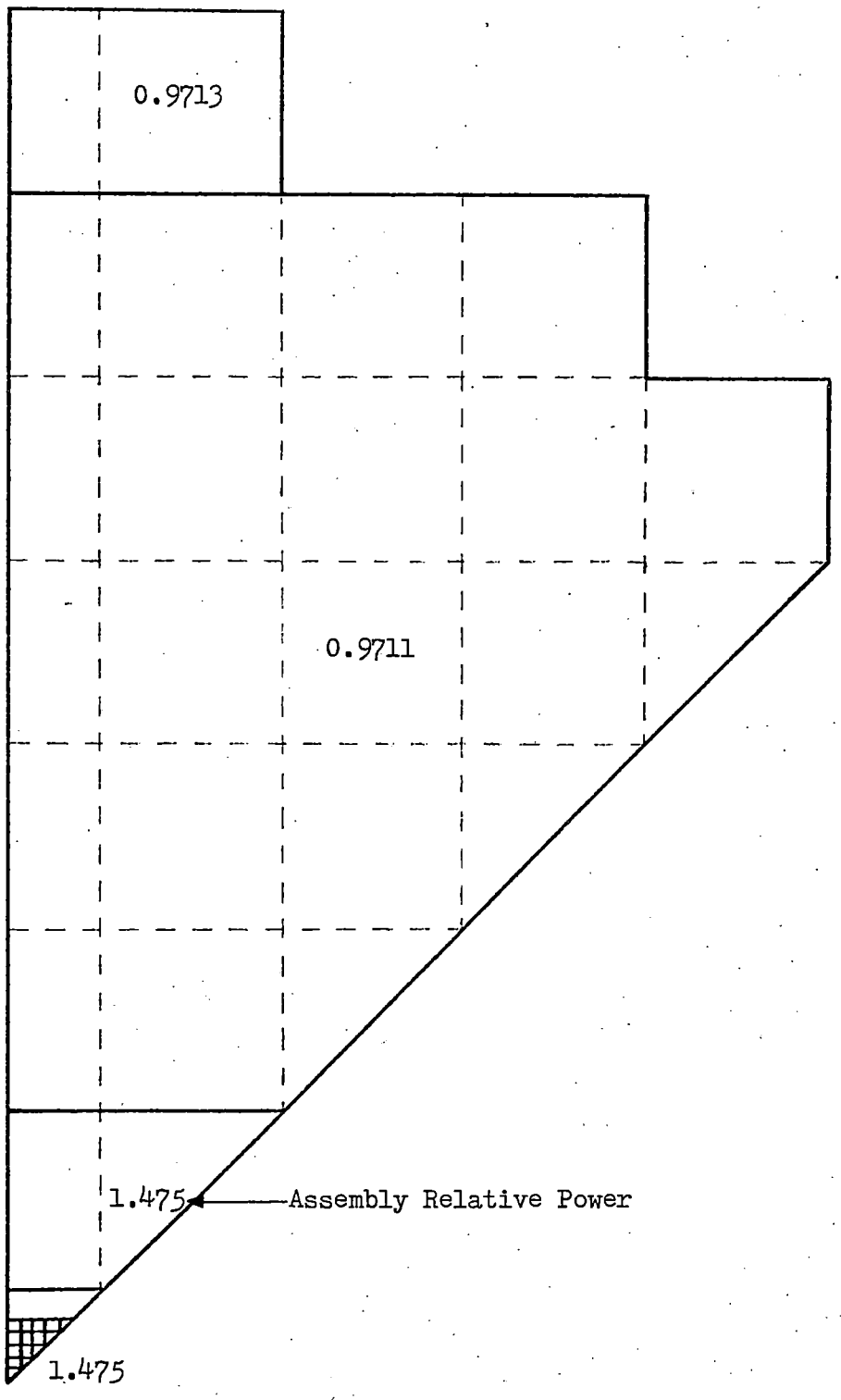

FIGURE 4-5

SUBCHANNEL POWER DISTRIBUTION, 53 CHANNEL MODEL
(LOW FLOW ASSUMPTION REANALYSIS)

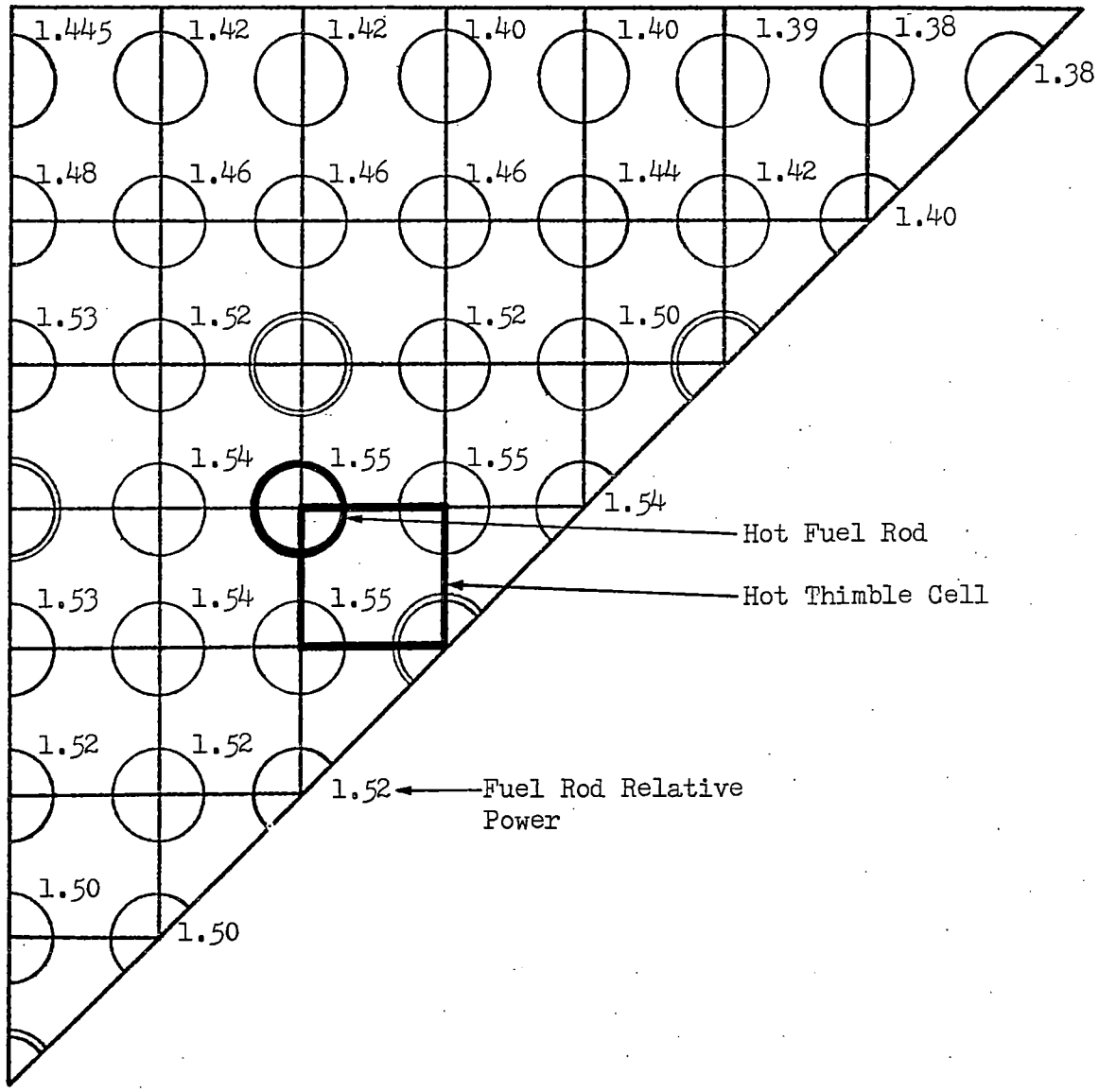

FIGURE 4-6

SUBCHANNEL POWER DISTRIBUTION, 19 CHANNEL MODEL
(LOW FLOW ASSUMPTION REANALYSIS)

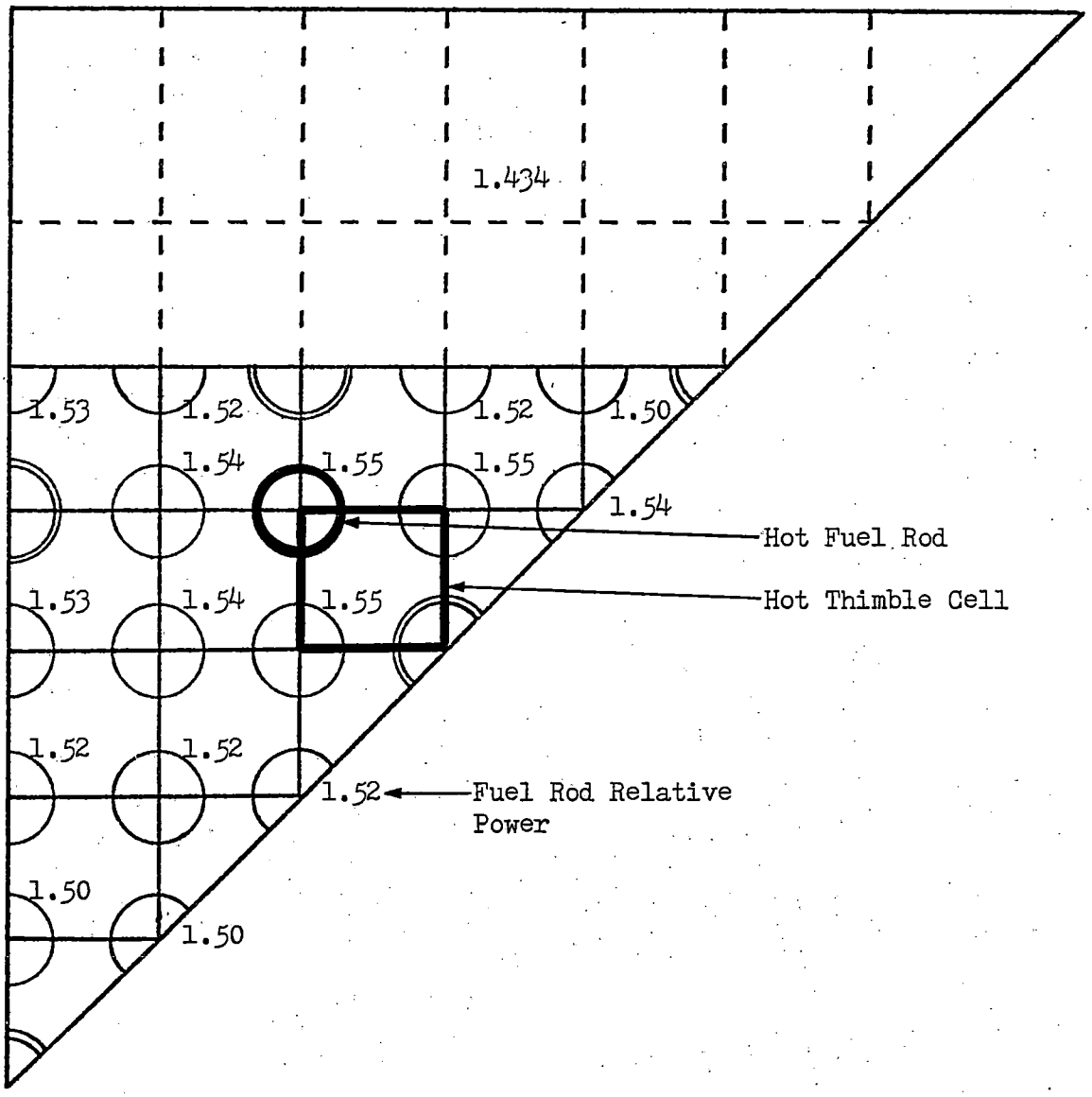

SECTION 5 - ENGINEERING UNCERTAINTIES

5.1 Introduction

After formulating the overall thermal-hydraulic representation of the core (see Sections 3 and 4), engineering uncertainties are then applied to account for manufacturing tolerances used in the fabrication of the fuel. These fabrication tolerances are assumed to occur in the hot channel, and they are therefore called hot channel factors. These factors and their application are discussed in detail in Section 5.2.

5.2 Hot Channel Factors

Three hot channel factors were used in all the DNB analyses described within this report. These factors consist of a pitch reduction, an engineering factor on the enthalpy rise ($F^E_{\Delta H}$), and an engineering factor on the heat flux (F^E_Q). The pitch reduction takes into account fuel rod spacing variations which may occur within the as-built fuel assembly. This reduced pitch is accounted for by modeling the hot channel with reduced gap spacings and a reduced flow area. Since a reduced flow area causes a greater pressure loss across the spacer grids,[25] this effect is taken into account by using increased grid loss coefficients. Table 5-1 lists the hydraulic data which was used in modeling the hot channel.

The engineering factor on the enthalpy rise ($F^E_{\Delta H}$) takes into account the effect of enrichment and density variations which may occur in as-built fuel rods. This factor is accounted for by increasing the relative power of the hot fuel rod. For all the DNB analyses described within this report, the relative power of the hot fuel rod was multiplied by a factor of 1.02.

The engineering factor on the heat flux (F_Q^E) takes into account the effect of enrichment, density, diameter, and eccentricity variations which may occur in as-built fuel pellets. This factor is accounted for by applying a heat flux spike on the hot fuel rod at the position of MDNBR. Before the heat flux spike can be applied, however, a thermal analysis must first be performed in order to determine the axial position of MDNBR. Based upon these results, the axial heat flux shape for the hot fuel rod is then adjusted to include a heat flux spike at the determined position. The spiked flux shape is included in a second thermal analysis from which the final results are obtained.

An engineering factor on the heat flux was applied to all the DNB analyses described within this report. However, it should be noted that recent spike DNB tests have shown that the actual spike effect on DNB is very small.[26] Based upon these tests, it was concluded that F_Q^E no longer had to be considered in DNB evaluations since its effect could be adequately accounted for in the DNBR design limit.

TABLE 5-1

HOT CHANNEL HYDRAULIC DATA

Hot Thimble Cell	
Pitch Reduction (inches)	0.0065
Reduced Flow Area (square inches)	0.1463
Reduced Fuel Rod to Fuel Rod Gap (inches)	0.1345
Reduced Fuel Rod to Thimble Tube Gap (inches)	0.0725
Increased Non-mixing Vane Grid Loss Coefficient	0.9866
Increased Mixing Vane Grid Loss Coefficient	1.2280
Hot Unit Cell	
Pitch Reduction (inches)	0.0065
Reduced Flow Area (square inches)	0.1698
Reduced Fuel Rod to Fuel Rod Gap (inches)	0.1345
Increased Non-mixing Vane Grid Loss Coefficient	0.7321
Increased Mixing Vane Grid Loss Coefficient	0.9110

SECTION 6 - THERMAL-HYDRAULIC MODEL VERIFICATION

6.1 Introduction

Three steady state and six transient DNB analyses were performed by VEPCO using the models and methods described in the preceeding sections. These analyses are listed in Table 6-1, and they are representative of those contained in the original Surry FSAR[8] and in subsequent licensing documents.[9,10,11,12] The later reanalyses update the FSAR and reflect the thermal-hydraulic design changes which were discussed in Section 4.2.

The analyses were performed in order to verify the calculational accuracy of the VEPCO Thermal-Hydraulic Model. For this reason, they were formulated to duplicate as closely as possible the original analyses contained in the above mentioned documents. Verification was obtained by comparing minimum DNBRs calculated using the VEPCO methods with those given in the licensing documents. These comparisons along with detailed descriptions of the analyses themselves are given in the following subsections.

TABLE 6-1

LISTING OF VEPCO VERIFICATION ANALYSES

FSAR[8] Analyses

Steady State at 100% Power

Excessive Load Increase Transient

Uncontrolled Control Rod Assembly Withdrawal at Power Transient

Complete Loss of Reactor Coolant Flow Transient

Densification[9]/Positive Moderator Temperature Coefficient[10,11] Reanalyses

Steady State at 112% Power

Uncontrolled Control Rod Assembly Withdrawal At Power Transient

Complete Loss of Reactor Coolant Flow Transient

Low Flow Assumption[12] Reanalyses

Steady State at 102% Power

Complete Loss of Reactor Coolant Flow Transient

6.2 FSAR Analyses

6.2.1 Introduction

The original FSAR analyses, which were performed using the VEPCO methods, consist of a steady state analysis at 100% power and three transient analyses. The radial power distributions for both the 53 and 19 channel models are shown in Figures 6-1 through 6-4. Relative flux values composing the axial power distribution are listed in Table 6-2. Reactor conditions and parameters which are applicable to the FSAR analyses are listed in Tables 6-3 and 6-4, respectively.

As identified in Table 6-4, the original Surry design included a high pressure DNB penalty. At the time, this penalty was applied for conservatism because of the relatively small amount of DNB data then available at higher operating pressures. DNBRs calculated using the VEPCO methods were thus adjusted so that they could be compared to those given in the FSAR. A DNBR divisor based upon the system pressure was calculated using the following relationship,

$$\text{DNBR Divisor} = 1.0 + 0.05 \left(\frac{P - 2000}{200}\right)$$

where P = system pressure, psia $(P \geq 2000)$

It should also be noted that the models developed by VEPCO for the FSAR group of analyses incorporate a unit cell as the hot channel (see Figures 6-3 and 6-4). These models reflect the fact that the unit cell had been assumed to be the limiting channel when the Surry units were first designed. All MDNBRs pertaining to this group of analyses are therefore based upon a hot unit cell.

6.2.2 Steady State Analysis at 100% Power

The Surry FSAR gives a MDNBR at nominal operating conditions of 1.97. Using the VEPCO methods along with the 53 channel model, a MDNBR of 1.94 was

calculated. A MDNBR of 1.94 was also calculated using the VEPCO methods along with the 19 channel model.

6.2.3 Excessive Load Increase Transient

An Excessive Load Increase transient is defined as a rapid increase in the steam generator steam flow that causes a power mismatch between the reactor core power and the steam generator load demand. The transient could result from either an administrative violation such as excessive loading by the operator or an equipment malfunction in the steam bypass control or turbine speed control. Since the Reactor Control System is designed to accommodate a 10 percent step load increase without a reactor trip, analyses are performed to demonstrate that in such cases the MDNBR does not fall below the design limit.

The case analyzed is a 10 percent step increase at EOL with the reactor at full power under manual control. Forcing functions of nuclear power, system pressure, and inlet temperature were obtained from the Surry FSAR. The inlet flow was assumed to be constant throughout the transient. (It should be noted that by using nuclear power instead of heat flux, the thermal lag of the fuel was neglected. This approximation is reasonable, however, since the nuclear power is changing slowly.) DNBR results, which were obtained using the 19 channel model, are shown in Figure 6-5. The FSAR shows a MDNBR of 1.55 while Vepco results show a MDNBR of 1.53.

6.2.4 Uncontrolled Control Rod Assembly Withdrawal at Power Transient

An Uncontrolled Control Rod Assembly Withdrawal at Power transient results in an increase in core heat flux. Since the heat extraction from the steam generator remains constant, there is a net increase in the reactor coolant temperature. Unless terminated by manual or automatic action, the power mismatch and resulting coolant temperature rise would eventually result in DNB.

The case analyzed is a slow control rod assembly withdrawal (2.0 x 10^{-5} ΔK/sec) from full power. Forcing functions of nuclear power, system pressure, and inlet temperature were obtained from the Surry FSAR. The inlet flow was assumed to be constant throughout the transient. Reactor trip on overtemperature ΔT occurs after approximately 48 seconds. DNBR results, which were obtained using the 19 channel model, are shown in Figure 6-6. The FSAR shows a MDNBR of 1.36 while VEPCO results show a MDNBR of 1.34.

6.2.5 Complete Loss of Reactor Coolant Flow Transient

A complete loss of forced reactor coolant flow may result from a simultaneous loss of electrical supplies to all reactor coolant pumps. If the reactor is at power at the time of the accident, the immediate effect of loss of coolant flow is a rapid increase in the coolant temperature. Unless terminated by reactor trip, the coolant temperature rise would result in DNB.

The case analyzed is a complete Loss of Reactor Coolant Flow transient with three pumps operating and the reactor at full power. Forcing functions of core average heat flux and core flow were obtained from the Surry FSAR. System pressure and inlet temperature were assumed constant throughout the transient. DNBR results, which were obtained using the 19 channel model, are shown in Figure 6-7. The FSAR shows a MDNBR of 1.46 while VEPCO results show a MDNBR of 1.48.

TABLE 6-2

AXIAL POWER DISTRIBUTION
FSAR ANALYSIS

$$F(z') = 1.72 \frac{\cos \frac{\pi z'(1.56523)}{12} - \cos \frac{\pi(1.56523)}{2}}{1 - \cos \frac{\pi(1.56523)}{2}}$$

Axial Flux Shape: 1.72 Cosine (144.0" Active Length)

z Axial Position (inches)	z' Fuel Position (feet)	z/156.0 Relative Position	F(z') Relative Flux
0.0	-	0.0000	0.0000
3.0	-6.0	0.0192	0.0000
10.2	-5.4	0.0654	0.1714
17.4	-4.8	0.1115	0.3776
24.6	-4.2	0.1577	0.6064
31.8	-3.6	0.2038	0.8438
39.0	-3.0	0.2500	1.0757
46.2	-2.4	0.2962	1.2881
53.4	-1.8	0.3423	1.4682
60.6	-1.2	0.3885	1.6052
67.8	-0.6	0.4346	1.6909
75.0	0.0	0.4808	1.7200
82.2	0.6	0.5269	1.6909
89.4	1.2	0.5731	1.6052
96.6	1.8	0.6192	1.4682
103.8	2.4	0.6654	1.2881
111.0	3.0	0.7115	1.0757
118.2	3.6	0.7577	0.8438
125.4	4.2	0.8038	0.6064
132.6	4.8	0.8500	0.3776
139.8	5.4	0.8962	0.1714
147.0	6.0	0.9423	0.0000
156.0	-	1.0000	0.0000

TABLE 6-3

REACTOR CONDITIONS, FSAR ANALYSIS

Steady State Analysis	
Power (% of nominal 2441 MWt)	100
Core Average Heat Flux (10^6 Btu/hr-ft^2)	0.196206
Inlet Temperature (^{o}F)	543
System Pressure (psia)	2250
Core Average Mass Velocity (10^6 lbm/hr-ft^2)	2.308
Transient Analysis (Initial Conditions)	
Power (% of nominal 2441 MWt)	102
Core Average Heat Flux (10^6 Btu/hr-ft^2)	0.200130
Inlet Temperature (^{o}F)	547
System Pressure (psia)	2220
Core Average Mass Velocity (10^6 lbm/hr-ft^2)	2.295

TABLE 6-4

PARAMETERS FOR FSAR ANALYSIS

$F_{\Delta H}$ (Hot Unit Cell)	1.58
F_Z	1.72
Hot Assembly Relative Power	1.432
Active Fuel Length (inches)	144.0
Reactor Flow (gpm at 543°F)	265,500
F_Q^E	1.03
$F_{\Delta H}^E$	1.02
Pitch Reduction (inches)	0.0065
CHF Correlation	W-3 with F-Factor
High Pressure DNB Penalty	1.05 per 200 psi above 2000 psia

FIGURE 6-1

ASSEMBLY POWER DISTRIBUTION, 53 CHANNEL MODEL
FSAR ANALYSIS

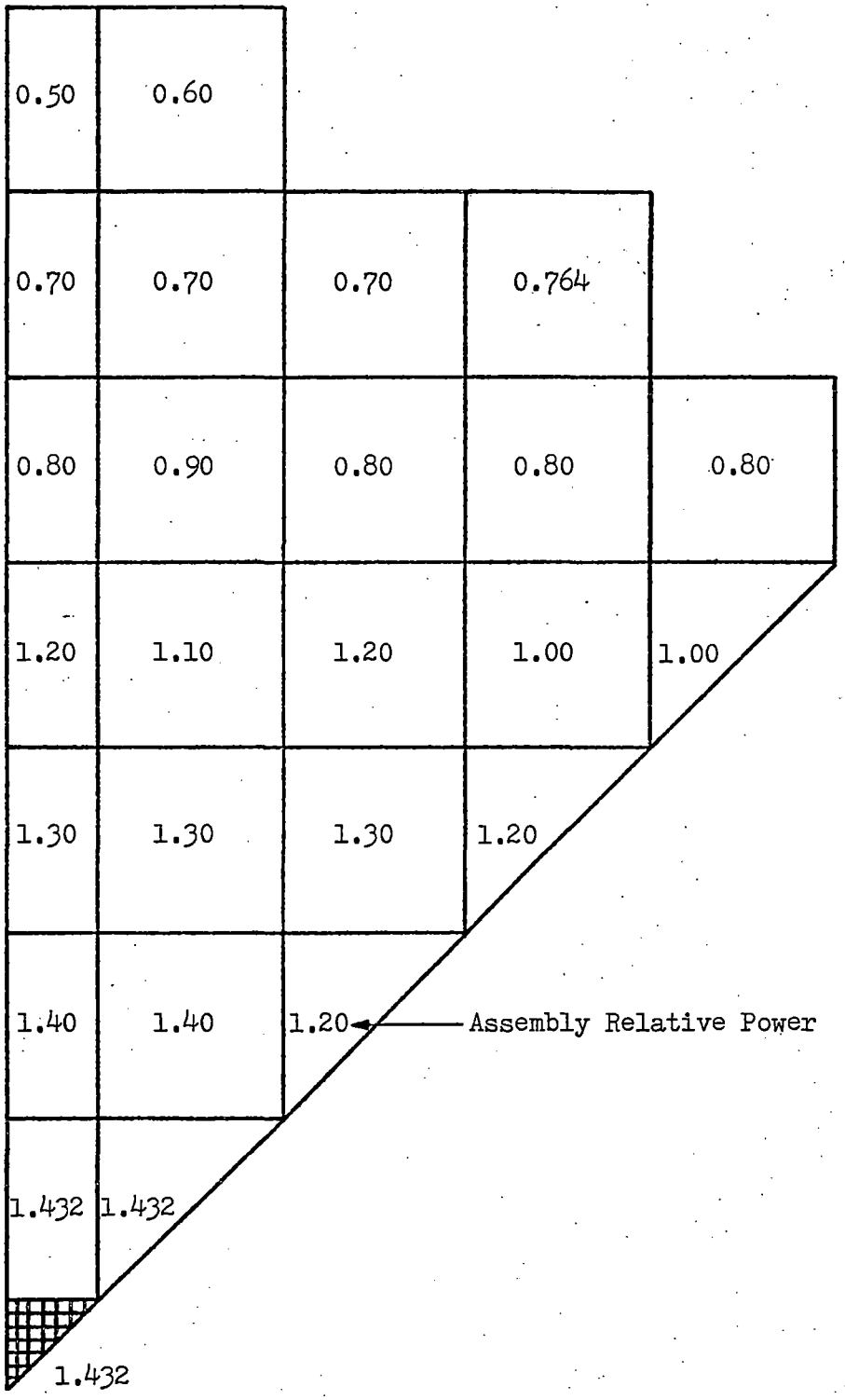

FIGURE 6-2

ASSEMBLY POWER DISTRIBUTION, 19 CHANNEL MODEL
FSAR ANALYSIS

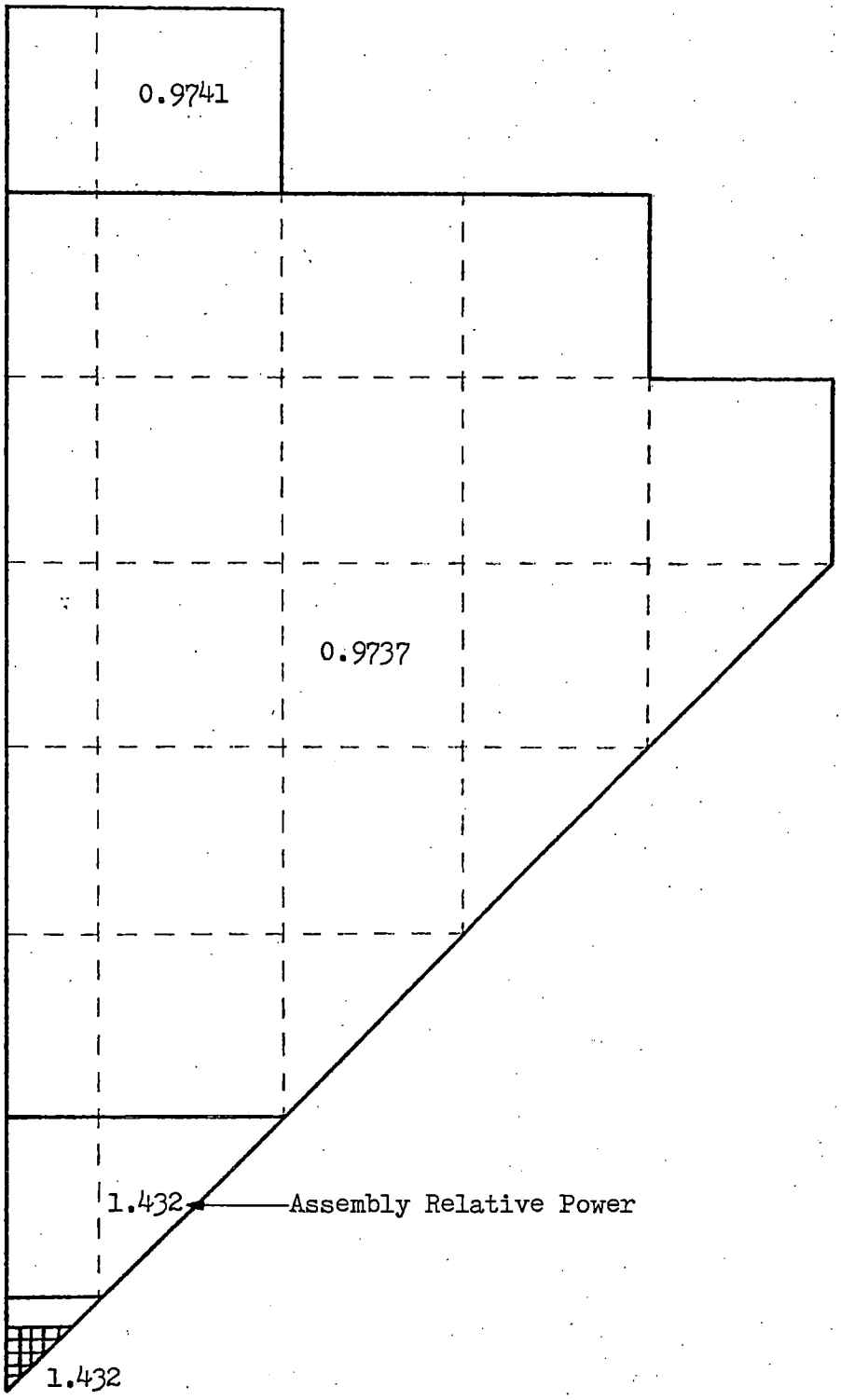

FIGURE 6-3

SUBCHANNEL POWER DISTRIBUTION, 53 CHANNEL MODEL
FSAR ANALYSIS

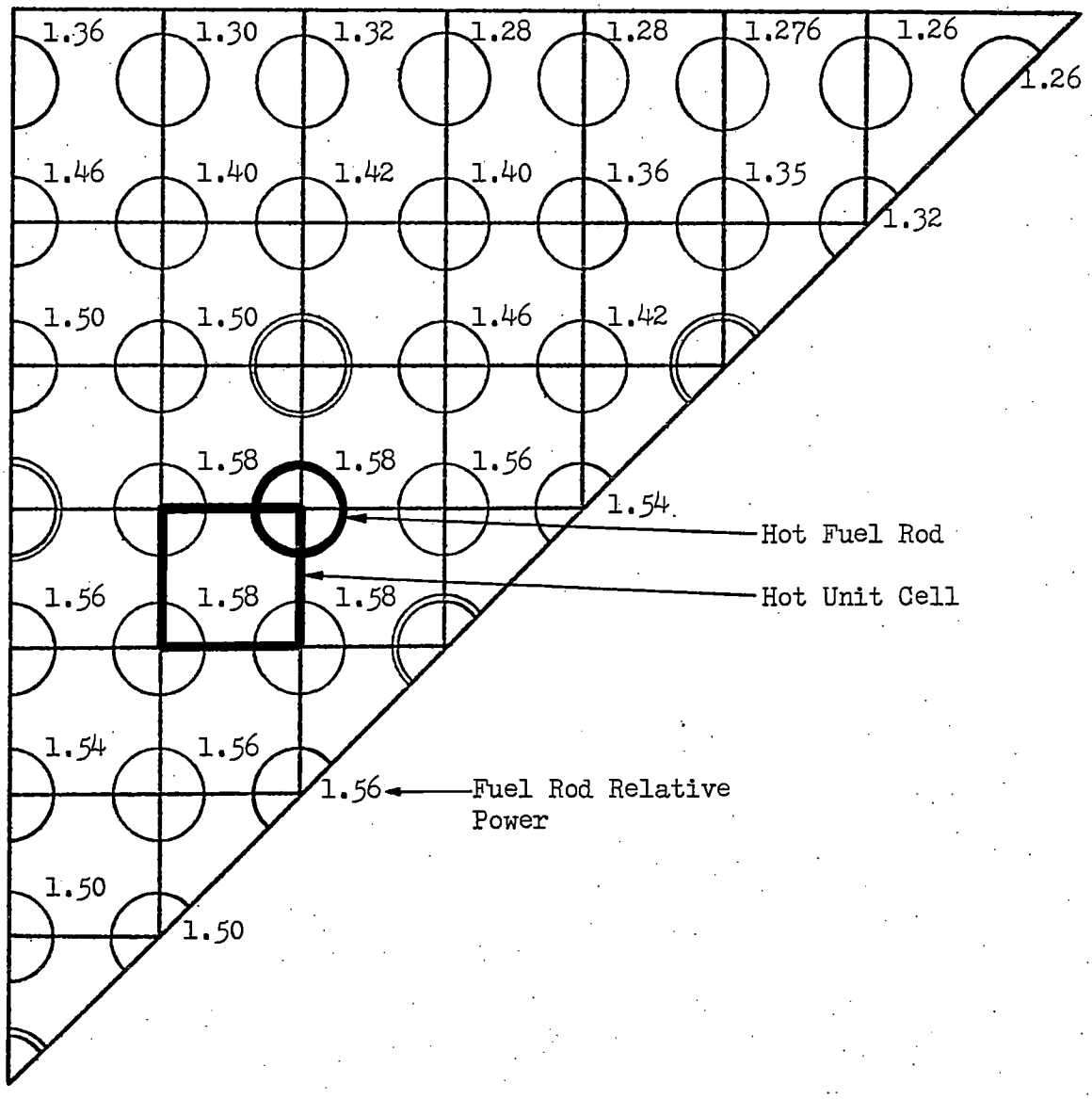

FIGURE 6-4

SUBCHANNEL POWER DISTRIBUTION, 19 CHANNEL MODEL
FSAR ANALYSIS

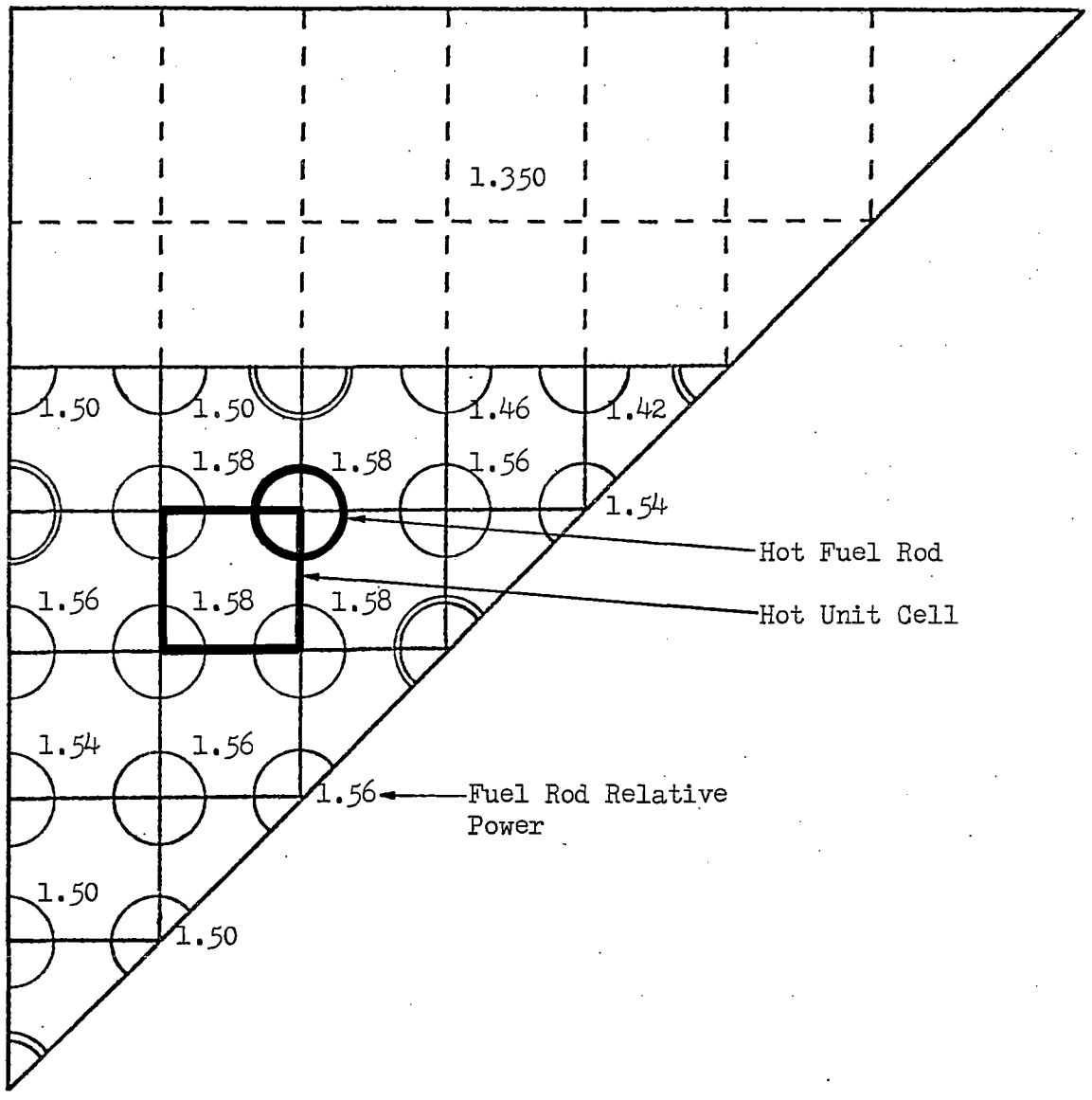

FIGURE 6-5

DNBR vs TIME
EXCESSIVE LOAD INCREASE TRANSIENT
FSAR ANALYSIS

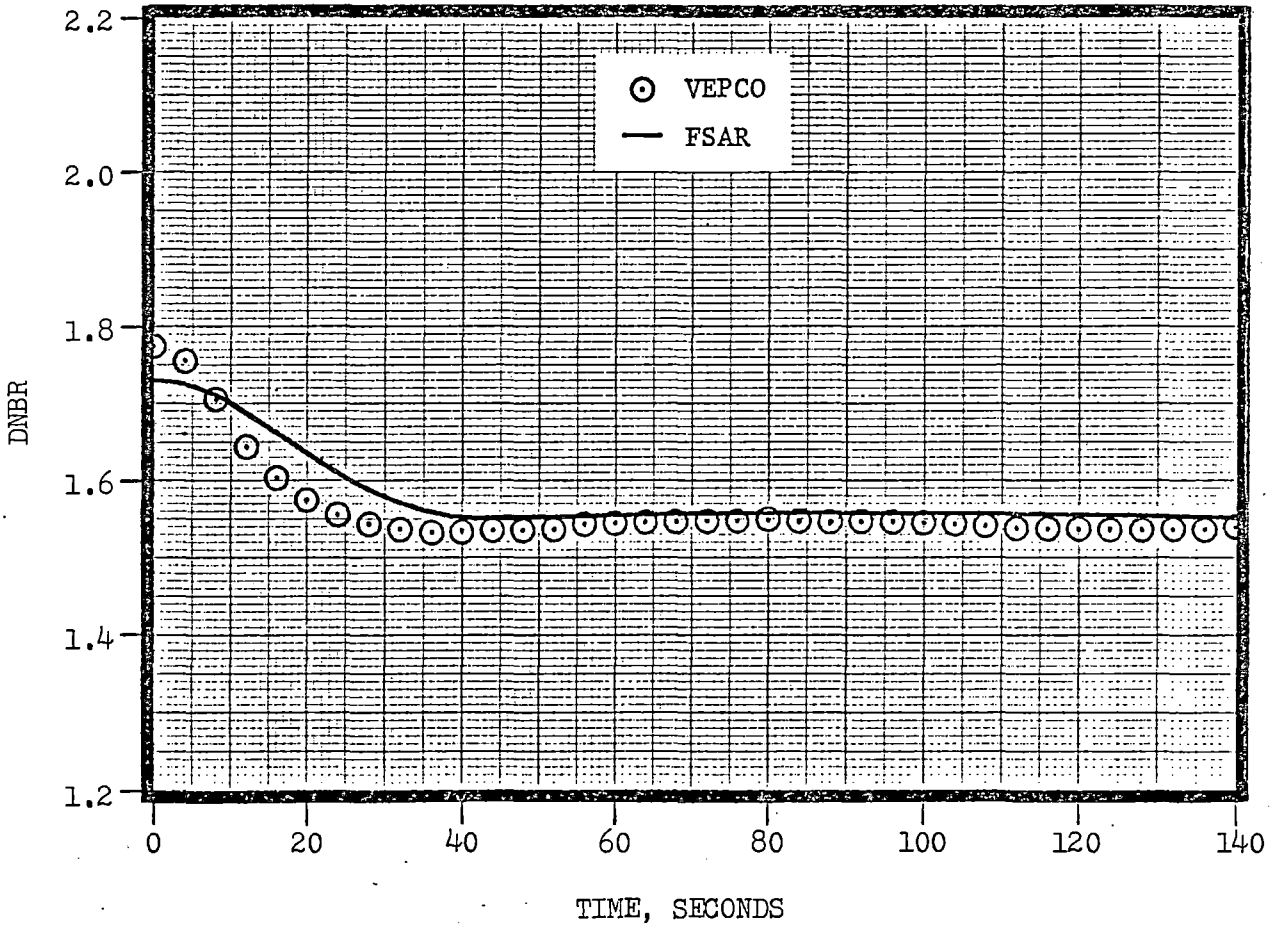

FIGURE 6-6

DNBR vs TIME
UNCONTROLLED CONTROL ROD ASSEMBLY WITHDRAWAL AT POWER TRANSIENT
FSAR ANALYSIS

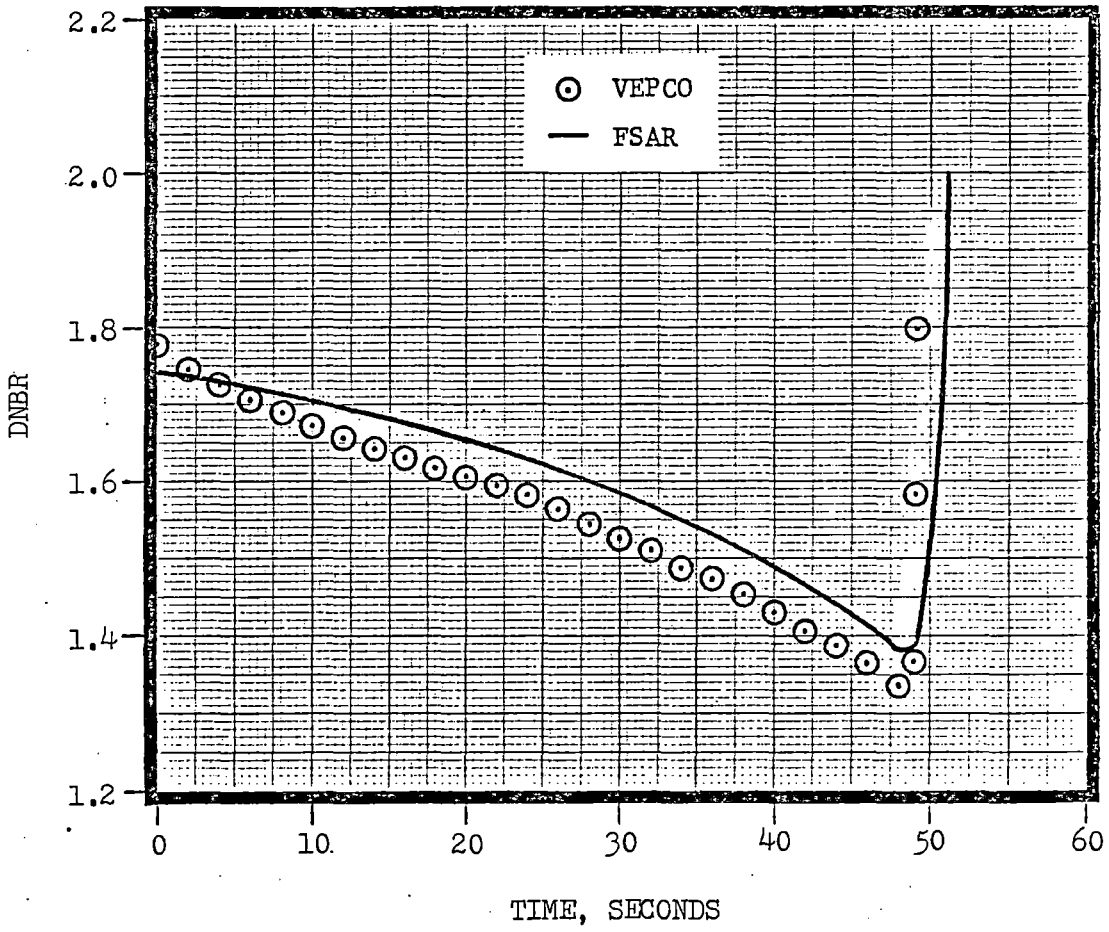

FIGURE 6-7

DNBR vs TIME
COMPLETE LOSS OF REACTOR COOLANT FLOW TRANSIENT
FSAR ANALYSIS

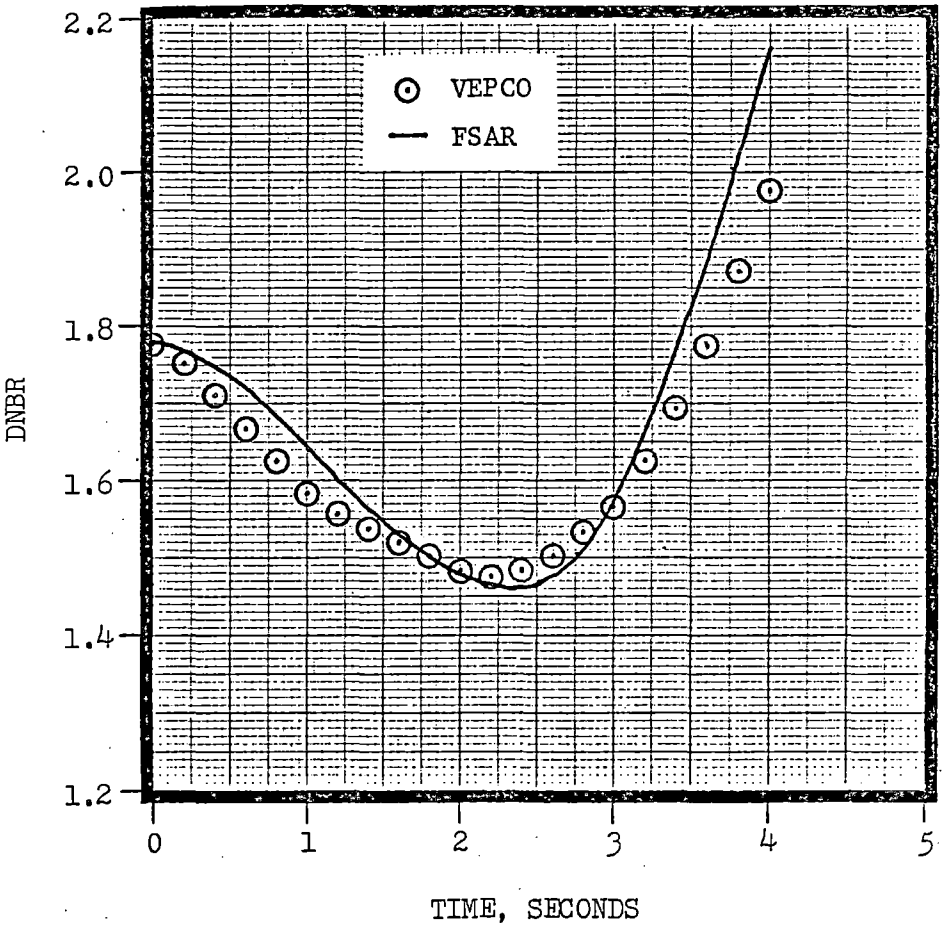

6.3 Densification/Positive Moderator Temperature Coefficient Reanalyses

6.3.1 Introduction

The densification and positive moderator temperature coefficient reanalyses, which were performed using the VEPCO methods, consist of a steady state analysis at 112% power and two transient analyses. The radial power distributions for both the 53 and 19 channel models are shown in Figures 6-8 through 6-11. Relative flux values composing the axial power distribution are listed in Table 6-5. Reactor conditions and parameters which are applicable to this group of reanalyses are listed in Tables 6-6 and 6-7, respectively.

As shown in Table 6-7, the parameters used in this group of reanalyses changed considerably when compared to the parameters used in the original FSAR analyses. Significant changes include the identification of the thimble cell as the limiting channel, the reduction of the radial and axial peaking factors, and the application of the coldwall and L-grid spacer factors to the W-3 CHF correlation. The fuel densification phenomenon was taken into account by reducing the active fuel length, increasing the magnitude of F_Q^E, and by applying a densification heat flux spike. For this group of reanalyses, F_Q^E and the densification heat flux spike were combined to form a single spike with a magnitude of approximately 1.244.

6.3.2 Steady State Analysis at 112% Power

The steady state analysis performed by VEPCO was based upon the safety limit curves which were revised to include the effects of fuel densification.[9] The safety limit curve for 2200 psia is shown in Figure 6-12. The horizontal segment of the curve, showing a constant average temperature, is an arbitrary (but conservative) upper limit such that the hot-leg temperature is less than the saturation temperature. The sloping segment of the curve represents the loci of points of thermal power, system pressure, and average temperature for

which the MDNBR is approximately 1.30. The reactor operating conditions for the steady state analysis were thus derived by choosing a point on the sloping segment of the curve. As depicted on the figure, at 112% power and 2200 psia, the average temperature is 588°F. This average temperature corresponds to an inlet temperature of approximately 554°F.

Using the VEPCO methods along with the 53 channel model, a MDNBR of 1.30 was calculated. Using the VEPCO methods along with the 19 channel model, a MDNBR of 1.27 was calculated. It should be noted that these two steady state analyses demonstrate the conservatism of the 19 channel model when reactor conditions are such that the resulting MDNBR approaches the design limit of 1.30. Under these conditions, a 19 channel steady state analysis will predict a MDNBR which is 2-3% lower than that predicted by a 53 channel analysis.

6.3.3 Uncontrolled Control Rod Assembly Withdrawal at Power Transient

As described in References 10 and 11, this transient was reanalyzed with an assumed positive moderator temperature coefficient. Margin to DNB was of concern since a positive moderator temperature coefficient would augment the mismatch in steam flow and core power. The particular case analyzed using the VEPCO methods is a slow rod withdrawal (2.3×10^{-5} $\Delta K/sec$) from full power. Forcing functions of heat flux, inlet temperature, and system pressure were obtained from Reference 11. The inlet flow was assumed to be constant throughout the transient. DNBR results, which were obtained using the 19 channel model, are shown in Figure 6-13. Reference 11 gives a MDNBR of 1.32 while VEPCO results show a MDNBR of 1.36.

6.3.4 Complete Loss of Reactor Coolant Flow Transient

As described in Reference 10, this transient was reanalyzed to determine the effect of an assumed positive moderator temperature coefficient on

the nuclear power and the resultant effect on DNBR. The case analyzed using the VEPCO methods is a complete Loss of Reactor Coolant Flow transient with three pumps operating and the reactor at full power. Forcing functions of core average heat flux and flow were obtained from Reference 10. System pressure and inlet temperature were assumed constant throughout the transient. Reference 10 states that the densification power spike penalty was removed when the reanalysis of this transient was performed (as justified in Reference 26). Accordingly, the densification heat flux spike was not included in the VEPCO analysis. DNBR results, which were obtained using the 19 channel model, are shown in Figure 6-14. Reference 10 gives a MDNBR of 1.54 while VEPCO results also show a MDNBR of 1.54.

TABLE 6-5

AXIAL POWER DISTRIBUTION
DENSIFICATION/POSITIVE MODERATOR TEMPERATURE COEFFICIENT REANALYSIS

$$F(z') = 1.55 \cos\left(\frac{\pi z'}{12.0201229}\right)$$

Axial Flux Shape: 1.55 Cosine (142.3" Active Length)

z Axial Position (inches)	z' Fuel Position (feet)	z/156.0 Relative Position	F(z') Relative Flux
0.00	-	0.0000	0.0000
2.98	-	0.0191	0.0000
3.00	-5.92916667	0.0192	0.0328
9.35	-5.4	0.0599	0.2461
16.55	-4.8	0.1061	0.4821
23.75	-4.2	0.1522	0.7062
30.95	-3.6	0.1984	0.9130
38.15	-3.0	0.2446	1.0975
45.35	-2.4	0.2907	1.2549
52.55	-1.8	0.3369	1.3816
59.75	-1.2	0.3830	1.4744
66.95	-0.6	0.4292	1.5310
74.15	0.0	0.4753	1.5500
81.35	0.6	0.5215	1.5310
88.55	1.2	0.5676	1.4744
95.75	1.8	0.6138	1.3816
102.95	2.4	0.6599	1.2549
110.15	3.0	0.7061	1.0975
117.35	3.6	0.7522	0.9130
124.55	4.2	0.7984	0.7062
131.75	4.8	0.8446	0.4821
138.95	5.4	0.8907	0.2461
145.30	5.92916667	0.9314	0.0328
145.31	-	0.9315	0.0000
156.00	-	1.0000	0.0000

TABLE 6-6

REACTOR CONDITIONS
DENSIFICATION/POSITIVE MODERATOR TEMPERATURE COEFFICIENT REANALYSIS

Steady State Analysis	
Power (% of nominal 2441 MWt)	112
Core Average Heat Flux (10^6 Btu/hr-ft^2)	0.222376
Inlet Temperature ($^\circ$F)	554
System Pressure (psia)	2200
Core Average Mass Velocity (10^6 lbm/hr-ft^2)	2.273
Transient Analysis (Initial Conditions)	
Power (% of nominal 2441 MWt)	102
Core Average Heat Flux (10^6 Btu/hr-ft^2)	0.202521
Inlet Temperature ($^\circ$F)	547
System Pressure (psia)	2220
Core Average Mass Velocity (10^6 lbm/hr-ft^2)	2.295

TABLE 6-7

PARAMETERS FOR DENSIFICATION/POSITIVE MODERATOR
TEMPERATURE COEFFICIENT REANALYSIS

$F_{\Delta H}$ (Hot Thimble Cell)	1.55
F_Z	1.55
Hot Assembly Relative Power	1.476
Active Fuel Length (inches)	142.3
Reactor Flow (gpm at 543°F)	265,500
F_Q^E	1.05
$F_{\Delta H}^E$	1.02
Pitch Reduction (inches)	0.0065
CHF Correlation	W-3 with F-Factor, Coldwall Factor, and L-Grid Spacer Factor (k_s = 0.046) (TDC = 0.019)
Densification Heat Flux Spike	1.185 Applied at the Axial Location of MDNBR

FIGURE 6-8

ASSEMBLY POWER DISTRIBUTION, 53 CHANNEL MODEL
DENSIFICATION/POSITIVE MODERATOR TEMPERATURE COEFFICIENT REANALYSIS

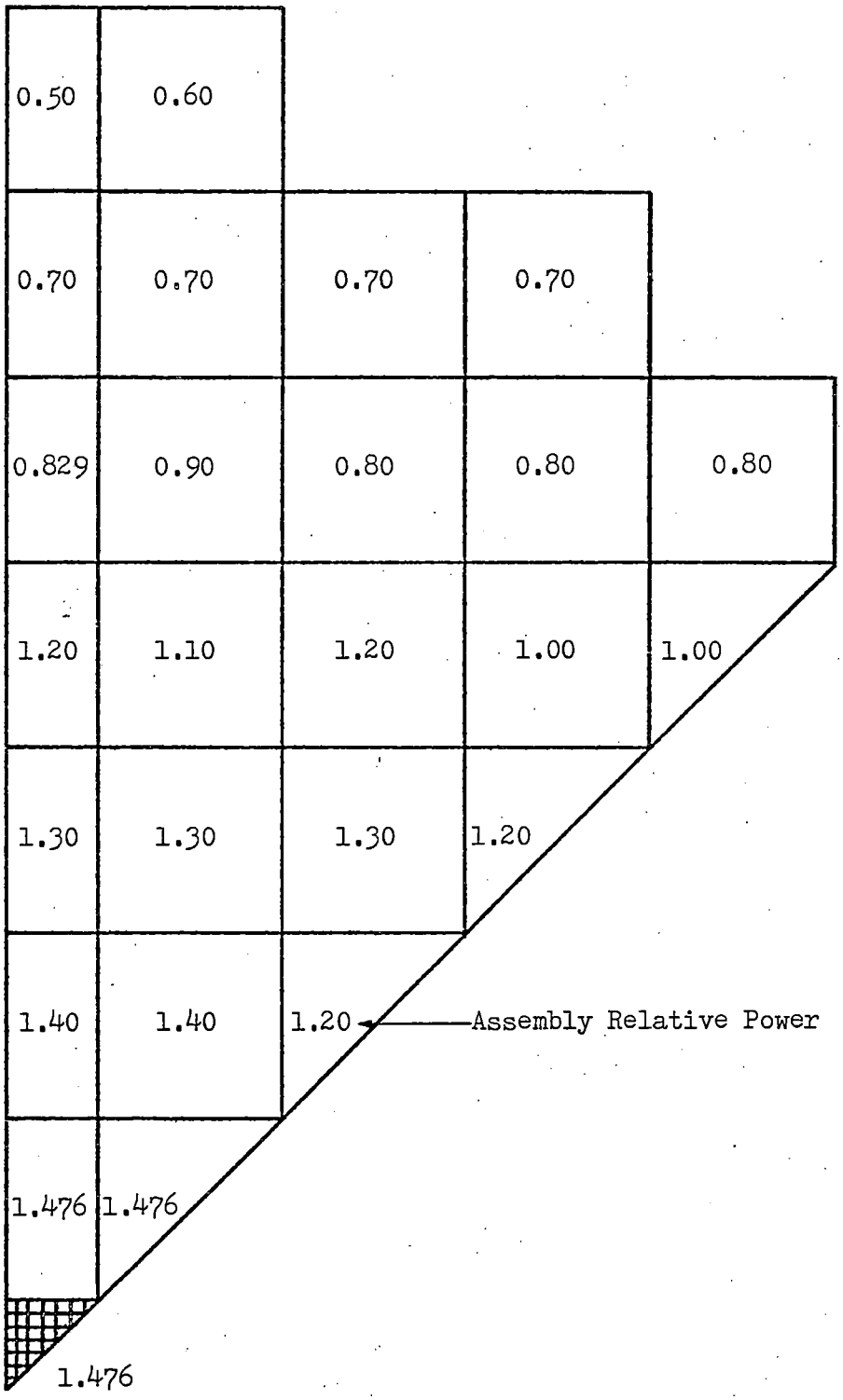

FIGURE 6-9

ASSEMBLY POWER DISTRIBUTION, 19 CHANNEL MODEL
DENSIFICATION/POSITIVE MODERATOR TEMPERATURE COEFFICIENT REANALYSIS

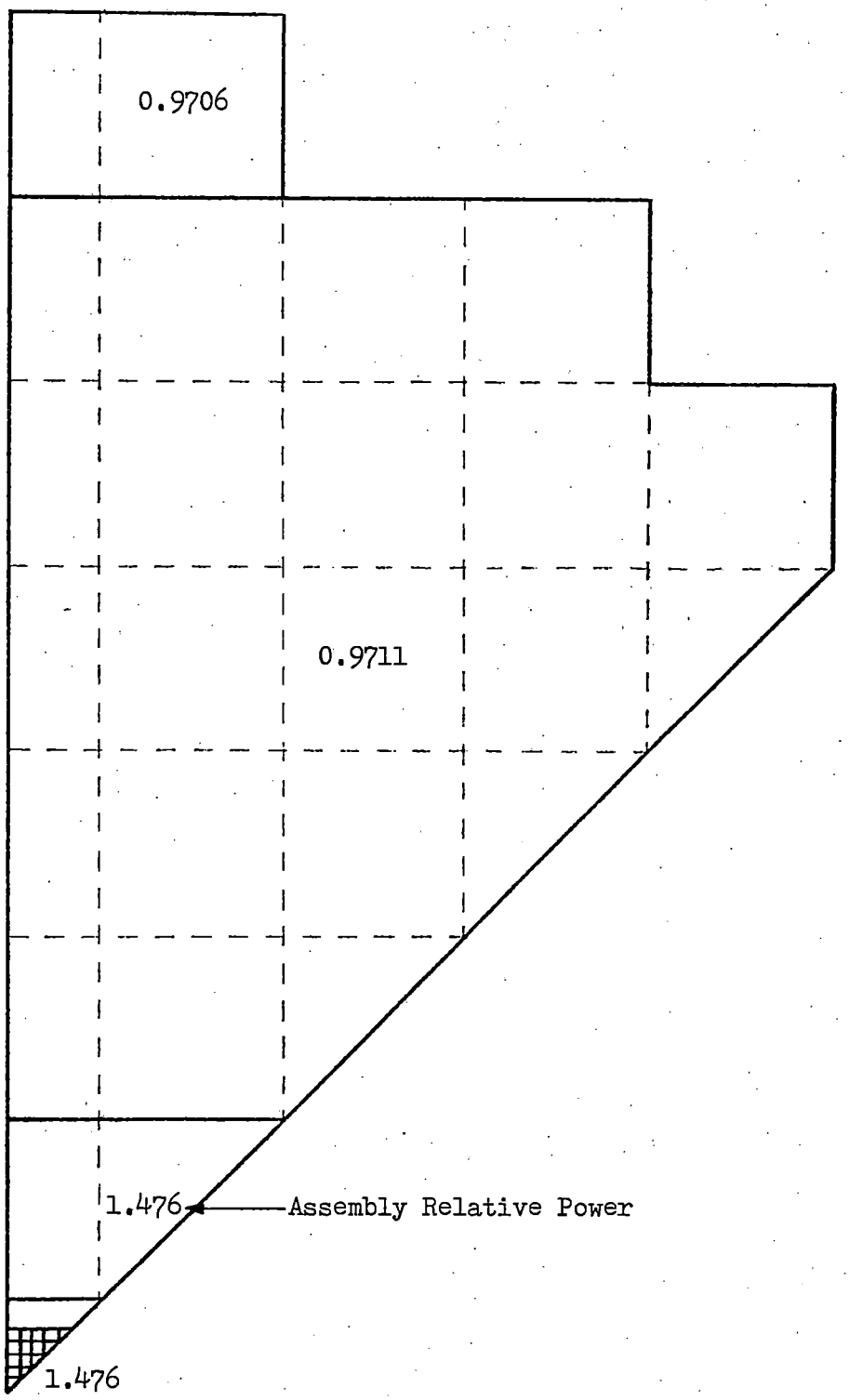

FIGURE 6-10

SUBCHANNEL POWER DISTRIBUTION, 53 CHANNEL MODEL
DENSIFICATION/POSITIVE MODERATOR TEMPERATURE COEFFICIENT REANALYSIS

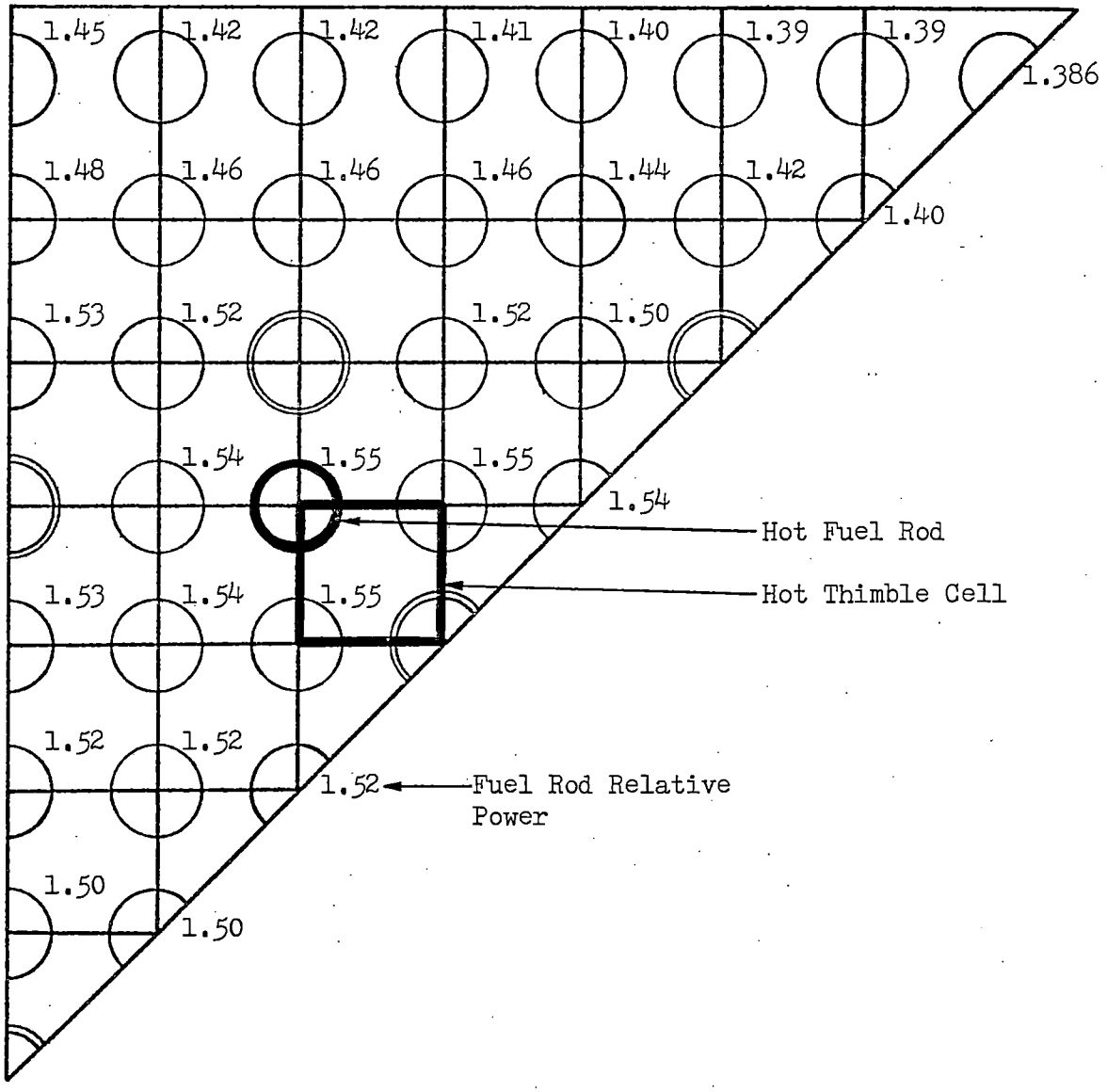

FIGURE 6-11

SUBCHANNEL POWER DISTRIBUTION, 19 CHANNEL MODEL
DENSIFICATION/POSITIVE MODERATOR TEMPERATURE COEFFICIENT REANALYSIS

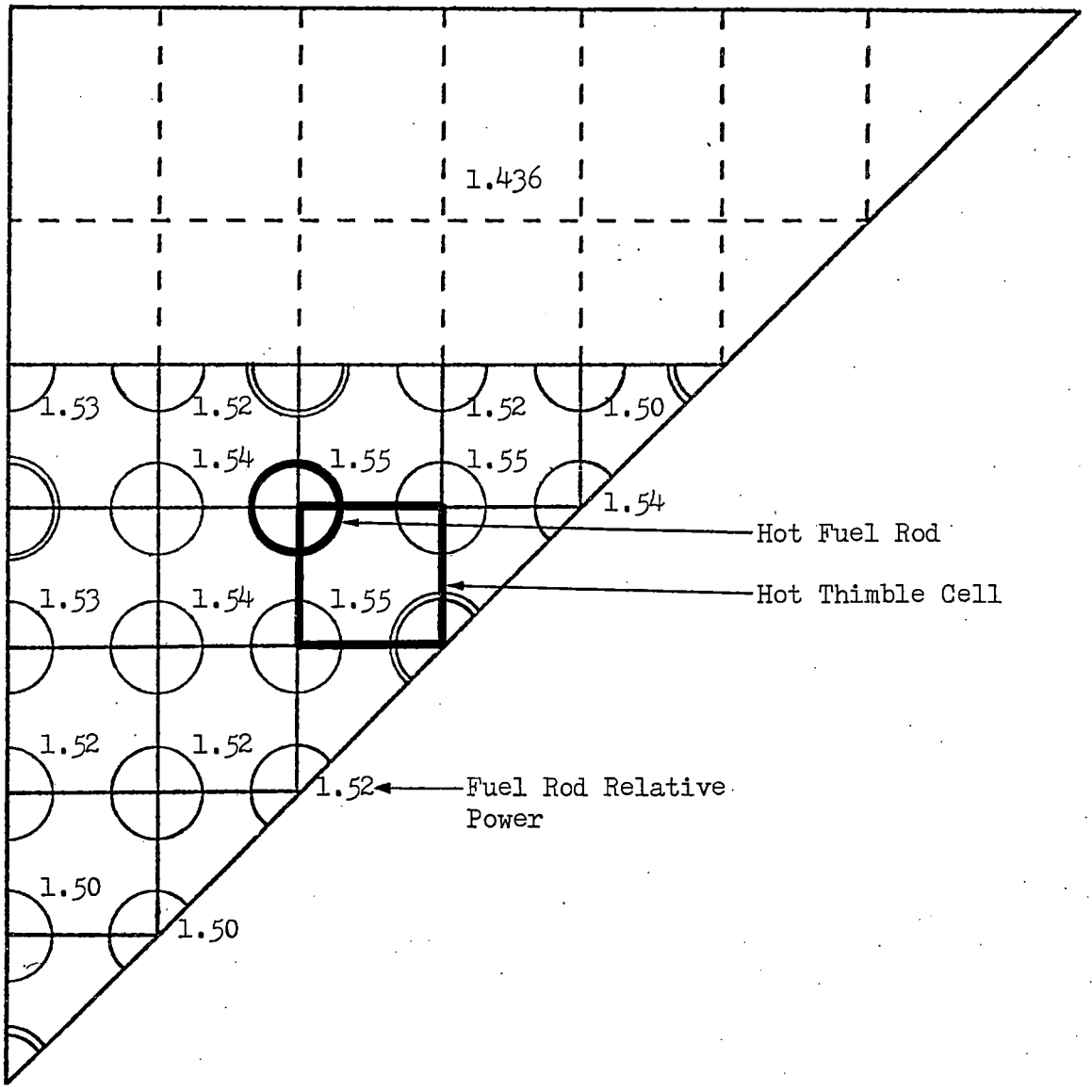

FIGURE 6-12

REACTOR CORE THERMAL AND HYDRAULIC SAFETY LIMIT
CURVE AT 2200 PSIA, THREE LOOP OPERATION, 100% FLOW

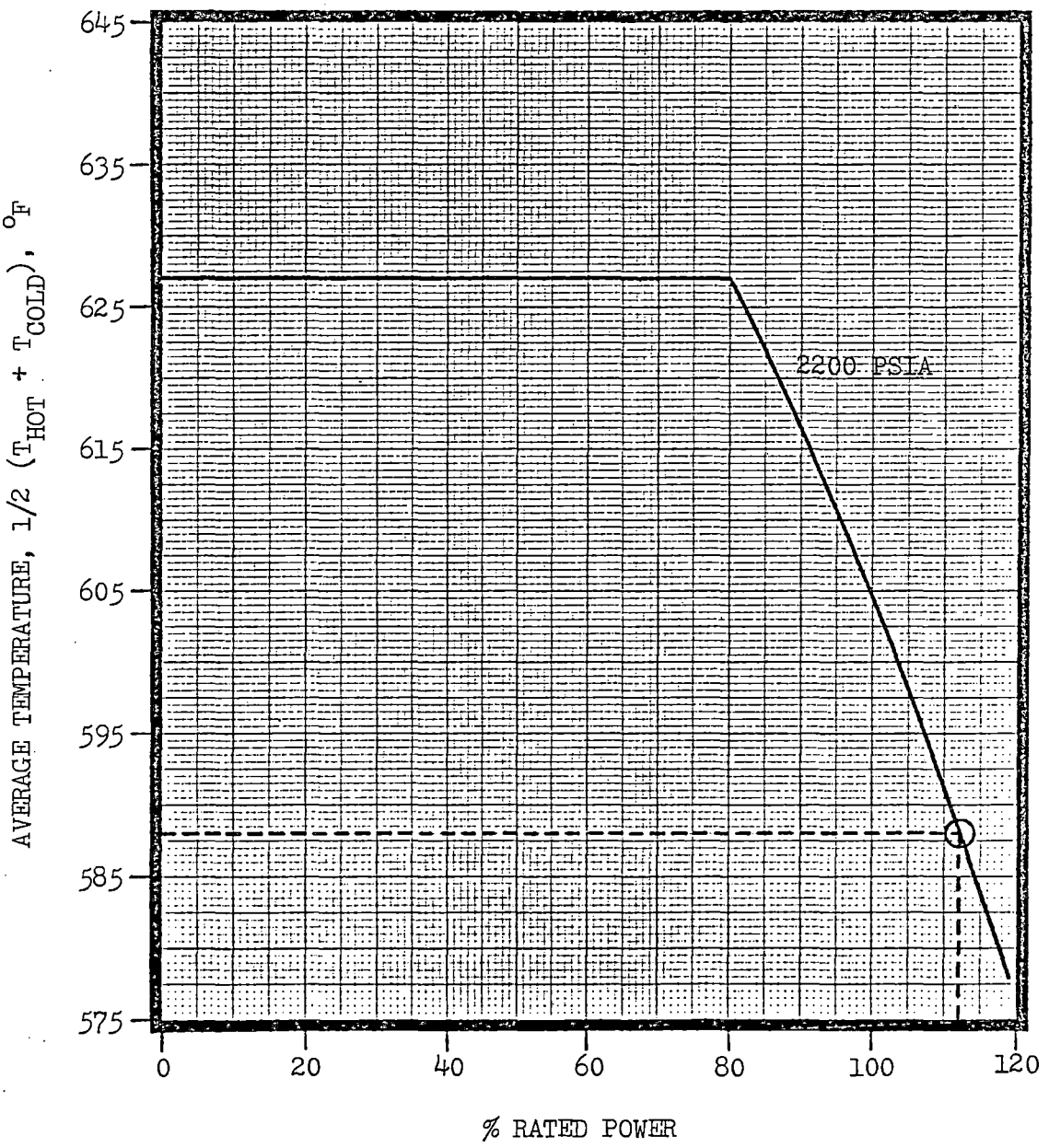

FIGURE 6-13

DNBR vs TIME
UNCONTROLLED CONTROL ROD ASSEMBLY WITHDRAWAL AT POWER TRANSIENT
POSITIVE MODERATOR TEMPERATURE COEFFICIENT REANALYSIS

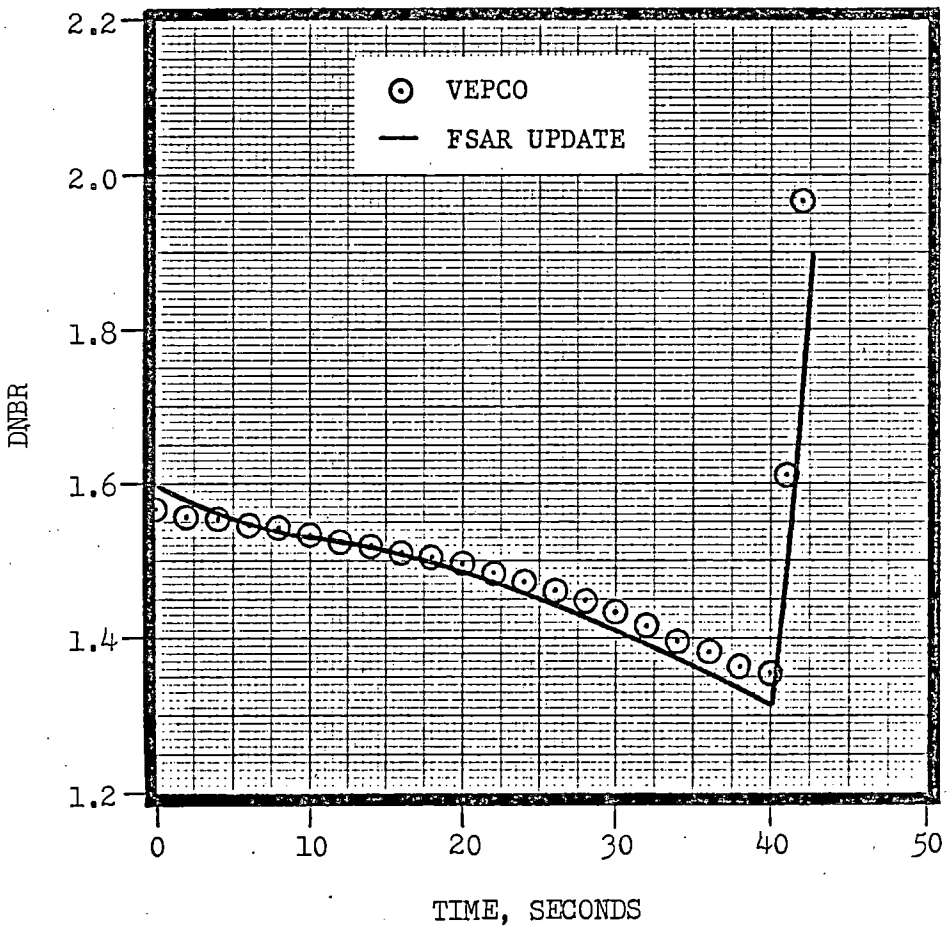

FIGURE 6-14

DNBR vs TIME
COMPLETE LOSS OF REACTOR COOLANT FLOW TRANSIENT
POSITIVE MODERATOR TEMPERATURE COEFFICIENT REANALYSIS

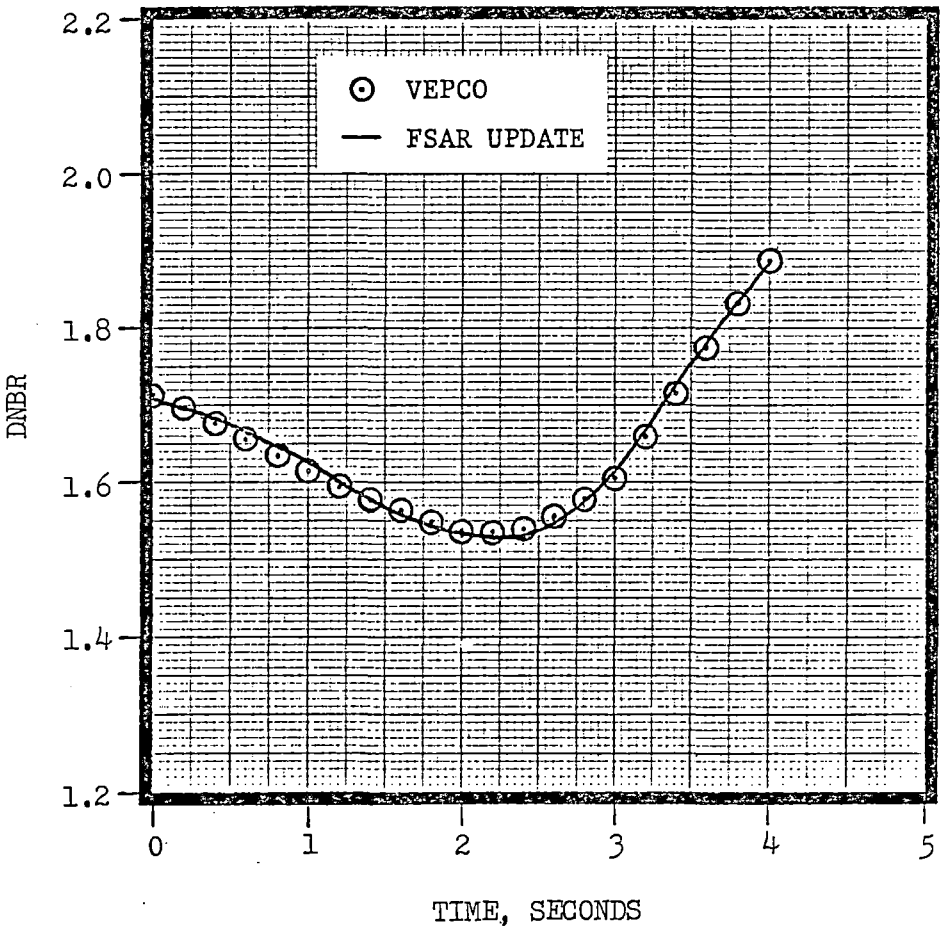

6.4 Low Flow Assumption Reanalyses

6.4.1 Introduction

The low flow assumption reanalyses, which were performed using the VEPCO methods, consist of a steady state analysis at 102% power and a complete Loss of Reactor Coolant Flow transient. The radial power distributions for both the 53 and 19 channel models have been previously described in Section 4 and are shown in Figures 4-3 through 4-6. The relative flux values composing the axial power distribution are listed in Table 4-1. Reactor conditions and parameters which are applicable to these reanalyses are listed in Tables 6-8 and 6-9, respectively.

As shown in Table 6-9, several parameters used in the low flow assumption reanalyses have again changed when compared to the parameters used in the densification reanalyses. Significant changes include the reduction in reactor flow to 90% of thermal design and the use of a revised densification model. The revised densification model is reflected in the active fuel length, in the engineering factor on the heat flux, F_Q^E, and in the elimination of the densification heat flux spike. It should be noted, however, that the effect of the densification heat flux spike for the Surry units was identified as a 7% DNB margin which was subsequently taken to partially offset the effects of fuel rod bowing on DNB.[27] Thus, DNBRs need to be reduced by 7% if they are obtained from analyses in which the densification heat flux spike has been eliminated.

6.4.2 Steady State Analysis at 102% Power

The steady state analysis performed by VEPCO was a state point analysis based upon the initial conditions of the complete Loss of Reactor Coolant Flow transient described in Reference 12. At the start of this transient, Reference 12 shows a MDNBR of approximately 1.50. Using the VEPCO methods

along with the 53 channel model a MDNBR of 1.49 was calculated. A MDNBR of 1.49 was also calculated using the VEPCO methods along with the 19 channel model. (Since the densification heat flux spike was not included in these analyses, all DNBRs were reduced by a factor of 1.07.)

6.4.3 Complete Loss of Reactor Coolant Flow Transient

The case analyzed using the VEPCO methods is a complete Loss of Reactor Coolant Flow transient with three pumps operating and the reactor at full power. Forcing functions of core average heat flux and core flow were obtained from Reference 12. System pressure and inlet temperature were assumed constant throughout the transient. Since the densification heat flux spike was not included in this analysis, all DNBRs were reduced by a factor of 1.07. DNBR results, which were obtained using the 19 channel model, are shown in Figure 6-15. Reference 12 gives a MDNBR of 1.33 while VEPCO results show a MDNBR of 1.35.

TABLE 6-8

REACTOR CONDITIONS
LOW FLOW ASSUMPTION REANALYSIS

Steady State Analysis	
Power (% of nominal 2441 MWt)	102
Core Average Heat Flux (10^6 Btu/hr-ft^2)	0.200687
Inlet Temperature (^{o}F)	547
System Pressure (psia)	2220
Core Average Mass Velocity (10^6 lbm/hr-ft^2)	2.065
Transient Analysis (Initial Conditions)	
Power (% of nominal 2441 MWt)	102
Core Average Heat Flux (10^6 Btu/hr-ft^2)	0.200687
Inlet Temperature (^{o}F)	547
System Pressure (psia)	2220
Core Average Mass Velocity (10^6 lbm/hr-ft^2)	2.065

TABLE 6-9

PARAMETERS FOR LOW FLOW ASSUMPTION REANALYSIS

$F_{\Delta H}$ (Hot Thimble Cell)	1.55
F_Z	1.55
Hot Assembly Relative Power	1.475
Active Fuel Length (inches)	143.6
Reactor Flow (gpm at 543°F)	238,950
F_Q^E	1.03
$F_{\Delta H}^E$	1.02
Pitch Reduction (inches)	0.0065
CHF Correlation	W-3 with F-Factor Coldwall Factor, and L-Grid Spacer Factor (k_s = 0.046) (TDC = 0.019)
Penalty to Partially Offset Rod Bow Effects on DNB	1.07

FIGURE 6-15

DNBR vs TIME
COMPLETE LOSS OF REACTOR COOLANT FLOW TRANSIENT
LOW FLOW ASSUMPTION REANALYSIS

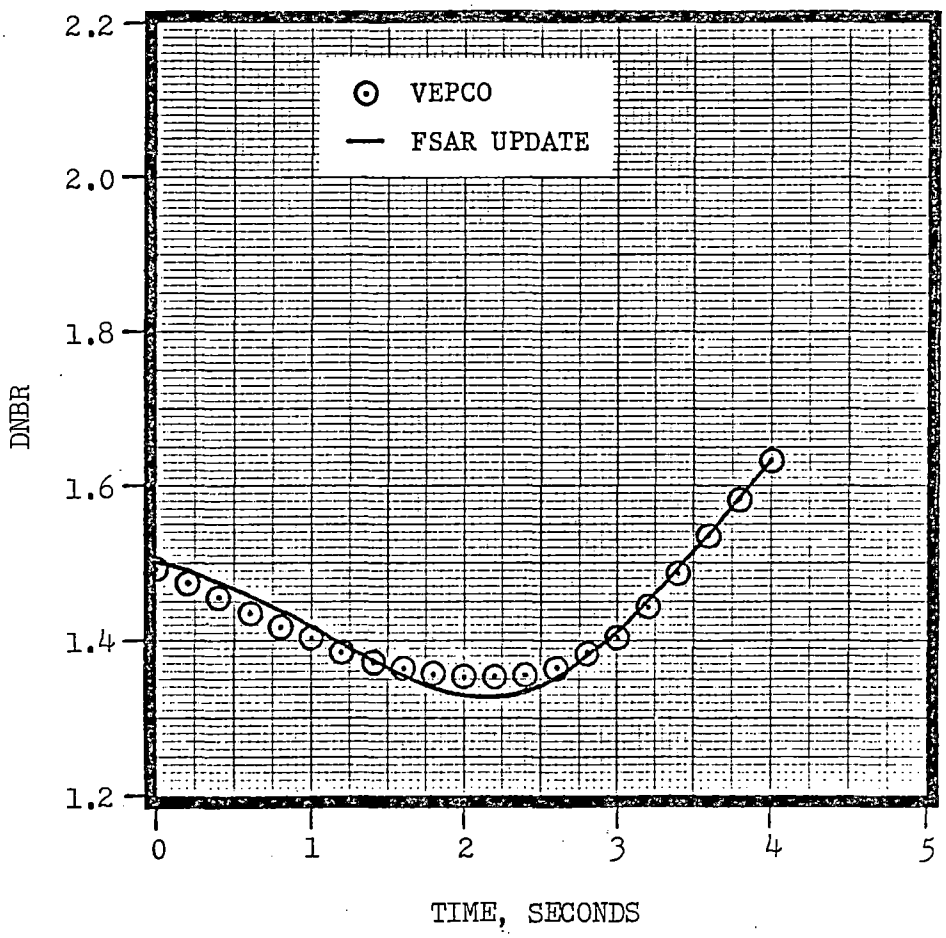

SECTION 7 - SUMMARY AND CONCLUSIONS

The Virginia Electric and Power Company (VEPCO) has developed the capability to perform core thermal-hydraulic analysis using the COBRA IIIC/MIT computer code. The basic models and methods have been documented in this report, and the accuracy of the capability has been established through comparisons with analyses which were used in the design and licensing of the Surry Nuclear Power Station. These comparisons, summarized in Table 7-1, show that the steady state and transient MDNBRs calculated using the VEPCO methods are in excellent agreement with those presented in the licensing documents. This agreement indicates that the capability can be used to provide design and licensing support for VEPCO reactor operations.

TABLE 7-1

SUMMARY OF COMPARISONS

	MINIMUM DNBR	
	FSAR	VEPCO
FSAR Analyses		
Steady State at 100% Power	1.97	1.94
Excessive Load Increase	1.55	1.53
Uncontrolled Control Rod Assembly Withdrawal at Power	1.36	1.34
Complete Loss of Reactor Coolant Flow	1.46	1.48
Densification/Positive Moderator Temperature Coefficient Reanalyses		
Steady State at 112% Power	1.30	1.30
Uncontrolled Control Rod Assembly Withdrawal at Power	1.32	1.36
Complete Loss of Reactor Coolant Flow	1.54	1.54
Low Flow Assumption Reanalyses		
Steady State at 102% Power	1.50	1.49
Complete Loss of Reactor Coolant Flow	1.33	1.35

SECTION 8 - REFERENCES

1. J. SHEFCHECK, "Application of the THINC Program to PWR Design," WCAP-7359-L, Westinghouse Electric Corporation (August, 1969), Proprietary.

2. L. E. HOCHREITER and H. CHELEMER, "Application of the THINC-IV Program to PWR Design," WCAP-8054, Westinghouse Electric Corporation (September, 1973), Proprietary.

3. B. R. HAO and J. M. ALCORN, "LYNX1 - Reactor Fuel Assembly Thermal-Hydraulic Analysis Code," BAW-10129, Rev. 1, Babcock and Wilcox (November, 1976).

4. "LYNX2 - Subchannel Thermal-Hydraulic Analysis Program," BAW-10130, Rev. 1, Babcock and Wilcox (April, 1977).

5. P. MORENO, J. LIU, E. KHAN, and N. TODREAS, "Steady-State Thermal Analysis of PWRs by a Simplified Method," Transactions of the American Nuclear Society, Vol. 26, p. 465 (June, 1977).

6. R. N. GUPTA, "Maine Yankee Core Thermal-Hydraulic Model Using COBRA-IIIC," YAEC-1102, Yankee Atomic Electric Company (June, 1976).

7. R. BOWRING and P. MORENO, "COBRA IIIC/MIT Computer Code Manual," prepared by MIT for EPRI (March, 1976).

8. Final Safety Analysis Report - Surry Power Station Units 1 and 2, Virginia Electric and Power Company (December, 1969).

9. "Fuel Densification - Surry Power Station Unit 1," WCAP-8012, Westinghouse Electric Corporation (December, 1972), Proprietary.

10. VEPCO (C. M. Stallings) to NRC (K. R. GOLLER) letter dated June 5, 1975, Serial No. 553, Docket Nos. 50-280 and 50-281.

11. VEPCO (C. M. STALLINGS) to NRC (B.C. RUSCHE) letter dated January 29, 1976, Serial No. 876, Docket Nos. 50-280 and 50-281.

12. VEPCO (C. M. STALLINGS) to NRC (E. G. CASE) letter dated August 9, 1977, Serial No. 344, Docket Nos. 50-280 and 50-281.

13. D. S. ROWE, "COBRA IIIC: A Digital Computer Program for Steady State and Transient Thermal-Hydraulic Analysis of Rod Bundle Nuclear Fuel Elements," BNWL-1695, Pacific Northwest Laboratory (March, 1973).

14. S.L. SMITH, "Void Fractions in Two-Phase Flow: A Correlation Based Upon an Equal Velocity Head Model," Proceedings of the Institution of Mechanical Engineers, Vol. 184, Part 1, No. 36, P. 647 (1969-70).

15. S. LEVY. "Forced Convection Subcooled Boiling - Prediction of Vapor Volumetric Fraction," GEAP-5157, General Electric Company (April, 1966).

16. J. P. WAGGENER, "Friction Factors for Pressure Drop Calculations," Nucleonics, Vol. 19, p. 145 (1961).

17. L. S. TONG, "Pressure Drop Performance of a Rod Bundle," Heat Transfer in Rod Bundles, ASME, pp. 57-69 (1968).

18. F. W. DITTUS and L. M. K. BOELTER, "Heat Transfer in Automobile Radiators of the Tubular Type," University of California Publications in Engineering Vol. 2, p. 443 (1930).

19. C. J. BAROCZY, "A systematic Correlation for Two-Phase Pressure Drop," NAA-SR-MEMO-11858, North American Aviation (March, 1966).

20. L. S. TONG, "Boiling Crisis and Critical Heat Flux," TID-25887, U. S. Atomic Energy Commission (1972).

21. W. H. JENS and P. A. LOTTES, "Analyses of Heat Transfer, Burnout, Pressure Drop, and Density Data for High Pressure Water," USAEC Report ANL-4627, Argonne National Laboratory (1951).

22. F. F. CADEK and F. E. MOTLEY, "Application of Modified Spacer Factor to L Grid Typical and Coldwall Cell DNB," WCAP-8030-A, Westinghouse Electric Corporation (January, 1975).

23. "PDQ7V2 for System 370," IBM-LB21-1467-0, International Business Machines Corporation (May, 1975).

24. Electric Power Research Institute Report EPRI CCM-5, "RETRAN - A Program for One-Dimensional Transient Thermal-Hydraulic Analysis of Complex Fluid Flow Systems," Energy Incorporated (December, 1978).

25. K. REHME, "Pressure Drop Correlations for Fuel Element Spacers," Nuclear Technology, Vol. 17, p. 15 (January, 1973).

26. J. M. HELLMAN, "Fuel Densification Experimental Results and Model for Reactor Application," WCAP-8219-A, Westinghouse Electric Corporation (March, 1975).

27. Westinghouse (C. EICHELDINGER) to NRC (V. STELLO) letter dated August 13, 1976, Serial No. NS-CE-1163.

APPENDIX A

VEPCO MODIFICATIONS ADDED TO THE COBRA IIIC/MIT COMPUTER CODE

The following list is a summary of the VEPCO modifications which were added to the original version of the COBRA IIIC/MIT computer code.

1. The code was modified so that the axial heat fluxes listed in the output were indicative of the corresponding axial positions. In the unmodified version of the code, the heat flux calculated for a particular axial position was actually the heat flux at the midpoint of the preceding axial interval. The code was further modified so that the heat added to the coolant over an axial interval was based upon the average of the heat fluxes at the beginning and the end of the interval.

2. The code was modified so that the calculation of the two-phase density in the subcooled void region was based upon the saturated vapor density and the subcooled liquid density. Analyses performed using the unmodified version of the code showed that the coolant density decreased abruptly at the axial position where subcooled voids were first formed. This discontinuity occurred because the two-phase density was calculated using the saturated liquid density when in reality the liquid was still subcooled. When the subcooled liquid density was used in the calculation, the discontinuity was eliminated. The code was further modified so that the subcooled void fractions could be retained for printout.

3. The code was double precisioned.

4. In order to better understand how the flow solution was progressing, the code was modified so that the largest convergence error was printed after each iteration.

5. The code was modified so that DNBRs were printed out by channel number instead of by rod number. Thus, minimum DNBRs and corresponding rod numbers were printed for each channel.

6. In order to perform more current DNB analyses, the W-3 L-grid and R-grid spacer factor correlations[22] were added to the code as options.

7. The code was modified to take into account the fraction of heat generated in the fuel and cladding. Because the heat fluxes calculated within the code are used for determining the heat added to the coolant, they are based upon the total heat generation rate (i.e., they include direct gamma heating of the coolant). These psuedo heat fluxes were therefore multiplied by the fraction of heat generated in the fuel and cladding in order to obtain actual heat fluxes. This adjustment was applied in the calculation of DNBRs, in the Jens and Lottes correlation[21] for determining the start of nucleate boiling, and in the Levy subcooled void model.[15]

8. The format of the DNBR data section was expanded so that at each axial position the actual heat flux, the fuel rod number, the F-factor, the cold-wall factor, the spacer grid factor, the critical heat flux, and the DNBR would be printed out for each channel.

9. The code was modified so that the calculation had to iterate at least twice before a converged solution would be accepted for printout.

10. The code was modified so that a variable damping factor could be input. The damping factor is used to obtain more rapid convergence.

11. The option was added so that different crossflow resistance coefficients and different mixing coefficients could be input and applied to the rod gaps.

12. The calculation using the Jens and Lottes correlation[21] for determining the start of nucleate boiling was corrected.

13. The code was modified so that from one to six different axial heat flux shapes could be input and applied to different fuel rods.

14. The code was modified to correct the calculation of the true (non-equilibrium) quality within the Levy subcooled void model.[15] Levy's paper states that the empirical constants used in developing the model were calculated using saturated liquid properties. Thus, to be consistent with the model, the code was modified so that the saturated liquid properties were used in calculating the true quality.

15. The code was modified so that all water properties (enthalpy, specific volume, viscosity, conductivity, and specific heat) were calculated using the HOH routines which were obtained from the PDQ7V2 computer code.[23]